Electronic Transactions on Numerical Analysis.
Volume 39, pp. 476-507, 2012.
Copyright © 2012, Kent State University.
ISSN 1068-9613.

ON THE MINIMIZATION OF A TIKHONOV FUNCTIONAL WITH A NON-CONVEX SPARSITY CONSTRAINT*

RONNY RAMLAU† AND CLEMENS A. ZARZER‡

Abstract. In this paper we present a numerical algorithm for the optimization of a Tikhonov functional with an ℓ_p-sparsity constraints and $p < 1$. Recently, it was proven that the minimization of this functional provides a regularization method. We show that the idea used to obtain these theoretical results can also be utilized in a numerical approach. In particular, we exploit the technique of transforming the Tikhonov functional to a more viable one. In this regard, we consider a surrogate functional approach and show that this technique can be applied straightforwardly. It is proven that at least a critical point of the transformed functional is obtained, which directly translates to the original functional. For a special case, it is shown that a gradient based algorithm can be used to reconstruct the global minimizer of the transformed and the original functional, respectively. Moreover, we apply the developed method to a deconvolution problem and a parameter identification problem in the field of physical chemistry, and we provide numerical evidence for the theoretical results and the desired sparsity promoting features of this method.

Key words. sparsity, surrogate functional, inverse problem, regularization

AMS subject classifications. 65L09, 65J22, 65J20, 47J06, 94A12

1. Introduction.

In this paper we consider a Tikhonov type regularization method for solving a (generally nonlinear) ill-posed operator equation

$$\mathcal{F}(x) = y \tag{1.1}$$

from noisy measurements y^δ with $\|y^\delta - y\| \leq \delta$. Throughout the paper we assume that $\mathcal{F}$ maps between sequence spaces, i.e.,

$$\mathcal{F} : D(\mathcal{F}) \subseteq \ell_p \to \ell_2.$$

Please note that operator equations between suitable separable function spaces such as L^p, Sobolev and Besov spaces, i.e.,

$$\tilde{\mathcal{F}} : D(\tilde{\mathcal{F}}) \subset X \to Y,$$

can be transformed to a sequence space setting by using a suitable basis or frames for $D(\tilde{\mathcal{F}})$ and $R(\tilde{\mathcal{F}})$. Assume that we are given some preassigned frames $\{\Phi^i_\lambda\}_{\lambda\in\Lambda_i, i=1,2}$ (Λ_i are countable index sets) for $D(\tilde{\mathcal{F}}) \subset X$, $R(\tilde{\mathcal{F}}) \subset Y$ with the associated frame operators T_1 and T_2. Then the operator $\mathcal{F} := T_2\tilde{\mathcal{F}}T_1^*$ maps between sequence spaces.

We are particularly interested in *sparse* reconstructions, i.e., the reconstruction of sequences with only few nonzero elements. To this end, we want to minimize the Tikhonov functional

$$\begin{aligned} J_{\alpha,p} : \ell_p &\to \mathbb{R} \\ x &\mapsto \begin{cases} \left\|F(x) - y^\delta\right\|_2^2 + \alpha \left\|x\right\|_p^p & x \in D(\mathcal{F}), \\ +\infty & \text{else,} \end{cases} \end{aligned} \tag{1.2}$$

---

*Received December 15, 2011. Accepted October 24, 2012. Published online on December 7, 2012. Recommended by G. Teschke. This work was supported by the grants FWF P19496-N18, FWF P20237-N14, and WWTF MA07-030.

†Institute of Industrial Mathematics, Johannes Kepler University Linz, Altenbergerstrasse 69, A-4040 Linz, Austria (`ronny.ramlau@jku.at`).

‡Johann Radon Institute for Computational and Applied Mathematics (RICAM), Austrian Academy of Sciences, Altenbergerstrasse 69, A-4040 Linz, Austria (`clemens.zarzer@ricam.oeaw.ac.at`).

where $\alpha > 0$, $0 < p \leq 1$, and

$$\|x\|_p^p = \sum_k |x_k|^p$$

is the (quasi-)norm of ℓ_p. The main aim of our paper is the development of an iterative algorithm for the minimization of (1.2), which is a non-trivial task due to the non-convexity of the quasi-norm and the nonlinearity of $\mathcal{F}$.

The reconstruction of the sparsest solution of an underdetermined system has already a long history, in particular in signal processing and more recently in compressive sensing. Usually the problem is formulated as

$$\tilde{x} := \underset{y=\Phi x}{\operatorname{argmin}} \|x\|_1, \tag{1.3}$$

where $y \in \mathbb{R}^m$ is given and $\Phi \in \mathbb{R}^{m,n}$ is a rank deficient matrix ($m < n$); see [19, 20]. Note that here the minimization of the ℓ_1-norm is used for the reconstruction of the sparsest solution of the equation $\Phi x = y$. Indeed, under certain assumptions on the matrix Φ, it can be shown that if there is a sparse solution, (1.3) really recovers it [9, 10, 17, 18]. Moreover, Gribonval and Nielsen [28] showed that for certain special cases, the minimization of (1.3) also recovers ℓ_p-minimizers with $0 < p < 1$. In this sense it seems that nothing is gained by considering an ℓ_p-minimization with $0 < p < 1$ instead of an ℓ_1-minimization, or equivalently, using an ℓ_p-penalty with $0 < p < 1$ in (1.2). However, we have to keep in mind that we are considering a different setting than the paper cited above. First of all, we are working in an infinite-dimensional setting, whereas the above mentioned Φ is a finite-dimensional matrix. Additionally, properties that guarantee the above cited results such as the so-called Restricted Isometry Property introduced by Candes and Tao [11, 10] or the Null Space Property [13, 16] are not likely to hold even for linear infinite-dimensional ill-posed problems, where, e.g., the eigenvalues of the operator converge to zero, not to speak of nonlinear operators. Recently, numerical evidence from a nonlinear parameter identification problem for chemical reaction systems has indicated that an ℓ_1-penalty in (1.2) fails to reconstruct a desired sparse parameter there, whereas stronger ℓ_p-penalties with $0 < p < 1$ achieve sparse reconstructions [30]. In the mentioned paper, the intention of the authors was the reconstruction of reduced chemical networks (represented by sparse parameter) from chemical measurements. Therefore, we conclude that the use of the stronger ℓ_p-penalties might be necessary in infinite-dimensional ill-posed problems if one wants a sparse reconstruction. In particular, algorithms for the minimization of (1.2) are needed.

There has been an increased interest in the investigation of the Tikhonov functional with sparsity constraints. First results on this matter were presented by Daubechies, Defriese, and De Mol [15]. The authors were in particular interested in solving linear operator equations. As a constraint in (1.2), they used a Besov semi-norm, which can be equivalently expressed as a weighted ℓ_p-norm of the wavelet coefficients of the functions with $p \geq 1$. In particular, that paper focuses on the analysis of a surrogate functional approach for the minimization of (1.2) with $p \geq 1$. It was shown that the proposed iterative method converges towards a minimizer of the Tikhonov functional under consideration. Additionally, the authors proposed a rule for the choice of the regularization parameter that guarantees the convergence of the minimizer x_α^δ of the Tikhonov functional to the solution as the data error δ converges to zero. Subsequently, many results on the regularization properties of the Tikhonov functional with sparsity constraints and $p \geq 1$ as well as on its minimization were published. In [39, 40], the surrogate functional approach for the minimization of the Tikhonov functional was generalized to nonlinear operator equations and in [23, 41] to multi-channel data, whereas in [5, 8] a conditional gradient method and in [29] a semi-smooth Newton method were proposed for the minimization. Further results on the topic of minimization and the respective algorithms can be found in [3, 6, 14]. The regularization properties with respect to different topologies and parameter choice rules were considered in [26, 31, 37, 38, 40, 41]. Please note again that the above cited results only consider the case $p \geq 1$. For the case $p < 1$, a first regularization result for some types of linear operators was presented in [31]. Recently in [24] and [45], the authors obtained general results on the regularization properties of the Tikhonov functional with a nonlinear operator and $0 < p < 1$. Concerning the minimization of (1.2) with $0 < p < 1$, to our knowledge no results are available in the infinite-dimensional setting. In the finite-dimensional setting, Daubechies et al. [16] presented an iteratively re-weighted least squares method for the solution of (1.3) that achieved local superlinear convergence. However, these results do not carry over to the minimization of (1.2), as the assumptions made in [16] (e.g., finite dimension, Null Space Property) do not hold for general inverse problems. Other closely related results for the finite-dimensional case can be found in [33, 34]. For a more general overview on sparse recovery, we refer to [42].

In this paper we present two algorithms for the minimization of (1.2) which are founded on the surrogate functional algorithm [15, 37, 39, 40] and the TIGRA algorithm [35, 36]. Based on a technique presented in [45] and on methods initially developed in [22], the functional (1.2) is nonlinearly transformed by an operator $\mathcal{N}_{p,q}$ to a new Tikhonov functional, now with an ℓ_q-norm as penalty and $1 < q \leq 2$. Due to the nonlinear transformation, the new Tikhonov functional involves a nonlinear operator even if the original problem is linear. Provided that the operator $\mathcal{F}$ fulfills some properties, it is shown that the surrogate functional approach at least reconstructs a critical point of the transformed functional. Moreover, the minimizers of the original and the transformed functional are connected by the transformation $\mathcal{N}_{p,q}$, and thus we can obtain a minimizer for the original functional. For the special case of $q = 2$, we show that the TIGRA algorithm reconstructs a global minimizer if the solution fulfills a smoothness condition. For the case $\mathcal{F} = \mathcal{I}$, where $\mathcal{I}$ denotes the identity, we show that the smoothness condition is always fulfilled for sparse solutions, whereas for $\mathcal{F} = \mathcal{A}$ with a linear operator $\mathcal{A}$, the finite basis injectivity (FBI) property is needed additionally.

The paper is organized as follows: in Section 2 we recall some results from [45] and introduce the transformation operator $\mathcal{N}_{p,q}$. Section 3 is concerned with some analytical properties of $\mathcal{N}_{p,q}$, whereas Section 4 investigates the operator $\mathcal{F} \circ \mathcal{N}_{p,q}$. In Section 5 we use the surrogate functional approach for the minimization of the transformed functional, and in Section 6 we introduce the TIGRA method for the reconstruction of a global minimizer. Finally in Section 7, we present numerical results for the reconstruction of a function from its convolution data and present an application from physical chemistry with a highly nonlinear operator. Both examples confirm our analytical findings and support the proposed enhanced sparsity promoting feature of the considered regularization technique.

Whenever it is appropriate, we omit the subscripts for norms, sequences, dual pairings, and so on. If not denoted otherwise, we consider the particular notions in terms of the Hilbert space ℓ_2 and the respective topology $\|\cdot\|_2$. Furthermore, we would like to mention that the subscript k shall indicate the individual components of an element of a sequence. The subscripts l and n are used for sequences of elements in the respective space or their components, e.g., $x_n = \{x_{n,k}\}_{k\in\mathbb{N}}$. Whenever referring to an entire sequence, we use $\{\cdot\}$ to denote the component-wise view. Iterates in terms of the considered algorithms are denoted by superscript l and n.

2. A transformation of the Tikhonov functional.

In [45] it was shown that (1.2) provides a regularization method under classical assumptions on the operator. The key idea was to transform the Tikhonov type functional by means of a superposition operator into a standard formulation. Below we give a brief summary on some results presented in [45] and consequently show additional properties of the transformation operator.

DEFINITION 2.1. *We denote by* $\eta_{p,q}$ *the function given by*

$$\begin{aligned} \eta_{p,q} : \mathbb{R} &\rightarrow \mathbb{R} \\ r &\mapsto \operatorname{sign}(r)\,|r|^{\frac{q}{p}}, \end{aligned}$$

for $0 < p \leq 1$ *and* $1 \leq q \leq 2$.

DEFINITION 2.2. *We denote by* $\mathcal{N}_{p,q}$ *the superposition operator given by*

$$\mathcal{N}_{p,q} : x \mapsto \{\eta_{p,q}(x_k)\}_{k\in\mathbb{N}},$$

where $x \in \ell_q$, $0 < p \leq 1$, *and* $1 \leq q \leq 2$.

PROPOSITION 2.3. *For all* $0 < p \leq 1$, $1 \leq q \leq 2$, $x \in \ell_q$, *and* $\mathcal{N}_{p,q}$ *as in Definition 2.2, it holds that* $\mathcal{N}_{p,q}(x) \in \ell_p$, *and the operator* $\mathcal{N}_{p,q} : \ell_q \rightarrow \ell_p$ *is bounded, continuous, and bijective.*

Using the concatenation operator

$$\begin{aligned} \mathcal{G} : \ell_q &\rightarrow \ell_2 \\ x &\mapsto \mathcal{F} \circ \mathcal{N}_{p,q}(x), \end{aligned}$$

one obtains the following two equivalent minimization problems.

PROBLEM 2.4. *Let* y^δ *be an approximation of the right-hand side of* (1.1) *with noise-level* δ, $\|y - y^\delta\| \leq \delta$, *and let* $\alpha > 0$. *Minimize*

$$J_{\alpha,p} = \begin{cases} \left\|\mathcal{F}(x_s) - y^\delta\right\|_2^2 + \alpha \left\|x_s\right\|_p^p & x_s \in D(\mathcal{F}), \\ +\infty & \textit{else}, \end{cases} \tag{2.1}$$

subject to $x_s \in \ell_p$ *for* $0 < p \leq 1$.

PROBLEM 2.5. *Let* y^δ *be an approximation of the right-hand side of* (1.1) *with noise-level* δ, $\|y - y^\delta\| \leq \delta$, *and let* $\alpha > 0$. *Determine* $x_s = \mathcal{N}_{p,q}(x)$, *where* x *minimizes*

$$\tilde{J}_{\alpha,q} = \begin{cases} \left\|\mathcal{G}(x) - y^\delta\right\|_2^2 + \alpha \left\|x\right\|_q^q & x_s \in D(\mathcal{G}), \\ +\infty & \textit{else}, \end{cases} \tag{2.2}$$

subject to $x \in \ell_q$ *and* $0 < p \leq 1$, $1 \leq q \leq 2$.

PROPOSITION 2.6. *Problem 2.4 and Problem 2.5 are equivalent.*

The paper [45] provides classical results on the existence of minimizers, stability, and convergence for the particular approach considered here using Tikhonov regularization. These results are obtained via the weak (sequential) continuity of the transformation operator.

3. Properties of the operator $\mathcal{N}_{p,q}$**.** Let us start with an analysis of the operator $\mathcal{N}_{p,q}$. The following proposition was given in [45]. We restate the proof as it is used afterward.

PROPOSITION 3.1. *The operator* $\mathcal{N}_{p,q} : \ell_q \rightarrow \ell_q$ *is weakly (sequential) continuous for* $0 < p \leq 1$ *and* $1 < q \leq 2$, *i.e.,*

$$x_n \overset{\ell_q}{\rightharpoonup} x \Longrightarrow \mathcal{N}_{p,q}(x_n) \overset{\ell_q}{\rightharpoonup} \mathcal{N}_{p,q}(x).$$

Here $\overset{X}{\rightharpoonup}$ *denotes the weak convergence with respect to the space* X.

Proof. We set $r = q/p{+}1$ and observe that $r \geq 2$. A sequence in ℓ_q is weakly convergent if and only if the coefficients converge and the sequence is bounded in the norm. Thus we conclude from the weak convergence of x_n that $\|x_n\|_q \le C$ and $x_{n,k} \to x_k$. As $r \ge q$, we have a continuous embedding of ℓ_r into ℓ_q, i.e.,

$$\|x_n\|_r \le \|x_n\|_q \le C,$$

which shows that also

$$x_n \overset{\ell_r}{\rightharpoonup} x$$

holds. The operator $(\mathcal{N}_{p,q}(x))_k = \operatorname{sgn}(x_k)|x_k|^{r-1}$ is the derivative of the function

$$f(x) = r^{-1} \cdot \|x\|_r^r,$$

or, in other words, $\mathcal{N}_{p,q}(x)$ is the *duality mapping* on ℓ_r with respect to the weight function

$$\varphi(t) = t^{r-1};$$

for more details on duality mappings we refer to [12]. Now it is a well known result that every duality mapping on ℓ_r is weakly (sequentially) continuous; see, e.g., [12, Proposition 4.14]. Thus we obtain

$$x_n \overset{\ell_r}{\rightharpoonup} x \Longrightarrow \mathcal{N}_{p,q}(x_n) \overset{\ell_r}{\rightharpoonup} \mathcal{N}_{p,q}(x).$$

Again, as $\mathcal{N}_{p,q}(x_n)$ is weakly convergent, we have $\{\mathcal{N}_{p,q}(x_n)\}_k \to \{\mathcal{N}_{p,q}(x)\}_k$. For $p \le 1$ and $q \ge 1$, it holds that $q \le q^2/p$, and thus we have $\|x\|_{q^2/p} \le \|x\|_q$. It follows that

$$\|\mathcal{N}_{p,q}(x_n)\|_q^q = \sum_k |x_{n,k}|^{q^2/p} = \|x_n\|_{q^2/p}^{q^2/p} \le \|x_n\|_q^{q^2/p} \le C^{q^2/p},$$

i.e., $\mathcal{N}_{p,q}(x_n)$ is also uniformly bounded with respect to the ℓ_q-norm and thus also weakly convergent. □

In the following proposition we show that the same result holds with respect to the weak ℓ_2-convergence.

PROPOSITION 3.2. *The operator $\mathcal{N}_{p,q} : \ell_2 \to \ell_2$ is weakly (sequentially) continuous with respect to ℓ_2 for $0 < p \le 1$ and $1 < q \le 2$, i.e.,*

$$x_n \overset{\ell_2}{\rightharpoonup} x \Longrightarrow \mathcal{N}_{p,q}(x_n) \overset{\ell_2}{\rightharpoonup} \mathcal{N}_{p,q}(x).$$

Proof. First of all, we have for $x \in \ell_2$ with $2q/p \ge 2$

$$\|\mathcal{N}_{p,q}(x)\|_2^2 = \sum_k |x_k|^{2q/p} = \|x\|_{2q/p}^{2q/p} \le \|x\|_2^{2q/p} < \infty,$$

i.e., $\mathcal{N}_{p,q}(x) \in \ell_2$ for $x \in \ell_2$. Setting again $r = q/p + 1$, the remainder of the proof follows along the lines of the previous one with $\|\cdot\|_q$ replaced by $\|\cdot\|_2$. □

Next we want to investigate the Fréchet derivative of $\mathcal{N}_{p,q}$. We need the following lemma in advance.

LEMMA 3.3. *The map $x \mapsto \operatorname{sgn}(x)\,|x|^\alpha$, $x \in \mathbb{R}$, is Hölder continuous with exponent α for $\alpha \in (0,1]$. Moreover, we have locally for $\alpha > 1$ and globally for $\alpha \in (0,1]$:*

$$\left|\operatorname{sgn}(x)\,|x|^\alpha - \operatorname{sgn}(y)\,|y|^\alpha\right| \le \kappa\,|x-y|^\beta\,, \tag{3.1}$$

where $\beta = \min(\alpha, 1)$.

Proof. As the problem is symmetric with respect to x and y, we may assume without loss of generality that $|x| \geq |y|$ and $|y| > 0$ as (3.1) immediately holds for $y = 0$. Let $\gamma \in \mathbb{R}_0^+$ such that $\gamma|y| = |x|$. For $\gamma \in [1, \infty)$ and $\alpha \in (0, 1]$, we have

$$(\gamma^\alpha - 1) \leq (\gamma - 1)^\alpha, \tag{3.2}$$

which can be obtained by comparing the derivatives of $(\gamma^\alpha - 1)$ and $(\gamma - 1)^\alpha$ for $\gamma > 1$ and by the fact that we have equality for $\gamma = 1$. Moreover, we have for $\gamma \in [0, \infty)$ and $\alpha \in (0, 1]$

$$(\gamma^\alpha + 1) \leq 2(\gamma + 1)^\alpha. \tag{3.3}$$

Since it is crucial that the constant in the Inequality (3.3) is independent of γ, we now give a proof of the factor 2 there. The ratio

$$\frac{(\gamma^\alpha + 1)}{(\gamma + 1)^\alpha}$$

is monotonously increasing for $\gamma \in (0, 1]$ and monotonously decreasing for $\gamma \in (1, \infty)$, which can be easily seen from its derivative. Hence, the maximum is attained at $\gamma = 1$ and given by $2^{1-\alpha}$, which yields

$$\frac{(\gamma^\alpha + 1)}{(\gamma + 1)^\alpha} \leq 2^{1-\alpha} \leq 2.$$

Consequently, we can conclude in the case of $x \cdot y > 0$ (i.e., $\mathrm{sgn}(x) = \mathrm{sgn}(y)$) that

$$\begin{aligned} |\mathrm{sgn}(x)|x|^\alpha - \mathrm{sgn}(y)|y|^\alpha| &= |\gamma^\alpha |y|^\alpha - |y|^\alpha| = |(\gamma^\alpha - 1)|y|^\alpha| \\ &\overset{(3.2)}{\leq} |(\gamma - 1)^\alpha |y|^\alpha| = |x - y|^\alpha, \end{aligned}$$

and for $x \cdot y < 0$ we have

$$\begin{aligned} |\mathrm{sgn}(x)|x|^\alpha - \mathrm{sgn}(y)|y|^\alpha| &= |\gamma^\alpha |y|^\alpha + |y|^\alpha| = |(\gamma^\alpha + 1)|y|^\alpha| \\ &\overset{(3.3)}{\leq} 2\,|(\gamma + 1)^\alpha |y|^\alpha| = 2\,|x - y|^\alpha. \end{aligned}$$

In the case of $\alpha > 1$, (3.1) holds with $\beta = 1$, which can be proven by the mean value theorem. For $\alpha > 1$, the function $f : x \mapsto \mathrm{sgn}(x)|x|^\alpha$ is differentiable and its derivative is bounded on any interval I. Hence, (3.1) holds for $|f'(\xi)| \leq \kappa, \xi \in I$, proving the local Lipschitz continuity. ☐

REMARK 3.4. In the following, Lemma 3.3 is used to uniformly estimate the remainder of a Taylor series. As shown in the proof, this immediately holds for $\alpha \in (0, 1]$. In the case of the Lipschitz estimate, this is valid only locally. However as all sequences in Proposition 3.5 are bounded and we are only interested in a local estimate, Lemma 3.3 can be applied directly.

PROPOSITION 3.5. *The Fréchet derivative of* $\mathcal{N}_{p,q} : \ell_q \to \ell_q$, $0 < p \leq 1$, $1 < q \leq 2$ *is given by the sequence*

$$\mathcal{N}'_{p,q}(x)h = \left\{ \frac{q}{p} |x_k|^{(q-p)/p} \cdot h_k \right\}_{k \in \mathbb{N}}.$$

Proof. Let $w := \min\left(\frac{q}{p} - 1, 1\right) > 0$. The derivative of $\eta_{p,q}(t) = |t|^{q/p}\operatorname{sgn}(t)$ is given by $\eta'_{p,q}(t) = \frac{q}{p}|t|^{(q-p)/p}$ and we define

$$\eta_{p,q}(t+\tau) - \eta_{p,q}(t) - \eta'_{p,q}(t)\tau := r(t,\tau),$$

where the remainder $r(t,\tau)$ can be expressed as

$$r(t,\tau) = \int_t^{t+\tau} \frac{q}{p}\frac{q-p}{p}(t+\tau-s)\operatorname{sgn}(s)|s|^{\frac{q}{p}-2}\,\mathrm{d}s.$$

In the considered ranges of p and q, the function $\eta_{p,q}$ is not twice differentiable. On this account, we derive the following estimate using the mean value theorem

$$\begin{aligned}\left|\int_t^{t+\tau} \frac{q}{p}\frac{q-p}{p}(t+\tau-s)\operatorname{sgn}(s)|s|^{\frac{q}{p}-2}\,\mathrm{d}s\right| &= \\ &= \left|\left[\frac{q}{p}(t+\tau-s)|s|^{q/p-1}\right]_t^{t+\tau} + \int_t^{t+\tau}\frac{q}{p}|t|^{q/p-1}\,\mathrm{d}s\right| \\ &= \left|\frac{q}{p}\tau\left(|\xi|^{q/p-1} - |t|^{q/p-1}\right)\right| \overset{(3.1)}{\leq} \kappa\frac{q}{p}|\tau|^{w+1},\end{aligned}$$

with $\xi \in (t, t+\tau)$ and by Lemma 3.3 with $\alpha = q/p - 1$, where κ is independent of τ; see Remark 3.4. Hence, we may write for $\|h\| = \|\{h_k\}\|$ sufficiently small

$$\begin{aligned}\left\|\mathcal{N}_{p,q}(x+h) - \mathcal{N}_{p,q}(x) - \mathcal{N}'_{p,q}(x)h\right\|_q^q = \|\{r(x_k,h_k)\}\|_q^q &= \sum_k |r(x_k,h_k)|^q \\ &\leq \sum_k\left(\frac{\kappa q}{p}\right)^q |h_k|^{q(w+1)} \\ &\leq \left(\frac{\kappa q}{p}\right)^q \max\left(\{|h_k|^{qw}\}\right)\sum_k |h_k|^q.\end{aligned}$$

Hence, we conclude that $\|\{r(x_k,h_k)\}\|_q / \|h\|_q \to 0$ for $\|h\|_q \to 0$ and obtain the formula for the derivative $\mathcal{N}'_{p,q}(x)h = \left\{\eta'_{p,q}(x_k)h_k\right\}_{k\in\mathbb{N}}$. $\square$

REMARK 3.6. Note that the result of Proposition 3.5 also holds in the case of the operator $\mathcal{N}_{p,q} : \ell_2 \to \ell_2$, as one can immediately see from the proof.

LEMMA 3.7. *The operator $\mathcal{N}'_{p,q}(x)$ is self-adjoint with respect to ℓ_2.*

Proof. We have $\langle \mathcal{N}'_{p,q}(x)h, z\rangle = \frac{q}{p}\sum|x_k|^{(q-p)/p}h_k z_k = \langle h, \mathcal{N}'_{p,q}(x)z\rangle$. $\square$

Please note that the Fréchet derivative of the operator $\mathcal{N}_{p,q}$ and its adjoint can be understood as (infinite-dimensional) diagonal matrices, that is,

$$\mathcal{N}'_{p,q}(x) = \operatorname{diag}\left(\left\{\frac{q}{p}|x_k|^{(q-p)/p}\right\}_{k\in\mathbb{N}}\right),$$

and $\mathcal{N}'_{p,q}(x)h$ is then a matrix-vector multiplication.

4. Properties of the concatenation operator $\mathcal{G}$.

The convergence of the surrogate functional approach, which will be applied to the transformed Tikhonov functional (2.2), relies mainly on some mapping properties of the operator $\mathcal{G} = \mathcal{F} \circ \mathcal{N}_{p,q}$. In the following, we assume that the operator $\mathcal{F}$ is Fréchet differentiable and $\mathcal{F}, \mathcal{F}'$ fulfill the following conditions.

Let $0 < p \leq 1$, $y \in \ell_2$ and let $x_n, x \in \ell_p$ and $x_n \rightharpoonup x$ with respect to the weak topology on ℓ_2. Moreover, for any bounded set $\Omega \subseteq D(\mathcal{F})$ there exists a $L > 0$ such that the following conditions hold:

$$F(x_n) \to F(x) \qquad \text{for } n \to \infty, \tag{4.1}$$

$$F'(x_n)^* y \to F'(x)^* y \qquad \text{for } n \to \infty, \tag{4.2}$$

$$\|F'(x) - F'(x')\|_2 \leq L\,\|x - x'\|_2 \qquad \text{for } x, x' \in \Omega. \tag{4.3}$$

Convergence and weak convergence in (4.1), (4.2) have to be understood with respect to ℓ_2. The main goal of this section is to show that the concatenation operator $\mathcal{G}$ is Fréchet differentiable and that this operator also fulfills the conditions given above. At first we obtain the following proposition.

PROPOSITION 4.1. *Let $\mathcal{F} : \ell_q \to \ell_2$ be strongly continuous with respect to ℓ_q, i.e.,*

$$x_n \overset{\ell_q}{\rightharpoonup} x \Longrightarrow \mathcal{F}(x_n) \overset{\ell_q}{\to} \mathcal{F}(x).$$

Then $\mathcal{F} \circ \mathcal{N}_{p,q}$ is also strongly continuous with respect to ℓ_q. If $\mathcal{F} : \ell_2 \to \ell_2$ is strongly continuous with respect to ℓ_2, then $\mathcal{F} \circ \mathcal{N}_{p,q}$ is also strongly continuous with respect to ℓ_2.

Proof. If $x_n \overset{\ell_q}{\rightharpoonup} x$, then by Proposition 3.1 also $\mathcal{N}_{p,q}(x_n) \overset{\ell_q}{\rightharpoonup} \mathcal{N}_{p,q}(x)$, and due to the strong continuity of $\mathcal{F}$ it follows that $\mathcal{F}(\mathcal{N}_{p,q}(x_n)) \to \mathcal{F}(\mathcal{N}_{p,q}(x))$. The second part of the proposition follows in the same way by Proposition 3.2. ☐

By the chain rule we immediately obtain the following result.

LEMMA 4.2. *Let $\mathcal{F} : \ell_q \to \ell_2$ be Fréchet differentiable. Then*

$$(\mathcal{F} \circ \mathcal{N}_{p,q})'(x) = \mathcal{F}'(\mathcal{N}_{p,q}(x)) \cdot \mathcal{N}'_{p,q}(x), \tag{4.4}$$

where the multiplication has to be understood as a matrix product. The adjoint (with respect to ℓ_2) of the Fréchet derivative is given by

$$((\mathcal{F} \circ \mathcal{N}_{p,q})'(x))^* = \mathcal{N}'_{p,q}(x) \cdot \mathcal{F}'(\mathcal{N}_{p,q}(x))^*. \tag{4.5}$$

Proof. Equation (4.4) is simply the chain rule. For the adjoint of the Fréchet derivative we obtain

$$\begin{aligned}
\langle((\mathcal{F} \circ \mathcal{N}_{p,q})'(x))u, z\rangle &= \langle \mathcal{F}'(\mathcal{N}_{p,q}(x)) \cdot \mathcal{N}'_{p,q}(x) \cdot u, z\rangle \\
&= \langle \mathcal{N}'_{p,q}(x) \cdot u, \mathcal{F}'(\mathcal{N}_{p,q}(x))^* \cdot z\rangle \\
&= \langle u, \mathcal{N}'_{p,q}(x) \cdot \mathcal{F}'(\mathcal{N}_{p,q}(x))^* z\rangle,
\end{aligned}$$

as $\mathcal{N}'_{p,q}(x)$ is self-adjoint. ☐

We further need the following result.

LEMMA 4.3. *Let $\mathcal{B} : \ell_q \to \ell_q$ be a diagonal linear operator (an infinite-dimensional diagonal matrix) with diagonal elements $b := \{b_k\}_{k\in\mathbb{N}}$. Then*

$$\|\mathcal{B}\|_{\ell_q \to \ell_q} \leq \|b\|_q.$$

Proof. The assertion follows from

$$\|\mathcal{B}\|^q_{\ell_q \to \ell_q} = \sup_{\|x\|_q^q \leq 1} \|\mathcal{B}x\|_q^q = \sup_{\|x\|_q^q \leq 1} \sum_k |b_k \cdot x_k|^q \leq \sum_k |b_k|^q. \qquad ☐$$

Hence, we may identify the operator $\mathcal{N}'_{p,q}(x_n)$ with the sequence of its diagonal elements and vice versa. Now we can verify the first required property.

PROPOSITION 4.4. *Let $x_n \rightharpoonup x$ with respect to ℓ_2, $z \in \ell_2$, and let q and p be such that $q \geq 2p$. Assume that*

$$(\mathcal{F}'(x_n))^* z \to (\mathcal{F}'(x))^* z \tag{4.6}$$

holds with respect to ℓ_2 for any weakly convergent sequence $x_n \to x$. Then we have as well

$$\left((\mathcal{F} \circ \mathcal{N}_{p,q})'(x_n)\right)^* z \to \left((\mathcal{F} \circ \mathcal{N}_{p,q})'(x)\right)^* z,$$

with respect to ℓ_2.

Proof. As $x_n \overset{\ell_2}{\rightharpoonup} x$, we have in particular $x_{n,k} \to x_k$ for a fixed k. The sequence $\mathcal{N}'_{p,q}(x_n)$ is given element-wise by

$$\frac{q}{p}|x_{n,k}|^{(q-p)/p} \to \frac{q}{p}|x_k|^{(q-p)/p},$$

and thus the coefficients of $\mathcal{N}'_{p,q}(x_n)$ converge to the coefficients of $\mathcal{N}'_{p,q}(x)$. In order to show weak convergence of the sequences, it remains to show that $\{\frac{q}{p}|x_{n,k}|^{(q-p)/p}\}$ stays uniformly bounded: we have

$$\|\mathcal{N}'_{p,q}(x_n)\|_2^2 = \left(\frac{q}{p}\right)^2 \sum_k \left(|x_{n,k}|^{(q-p)/p}\right)^2 .$$

As $q \geq 2p$ and $\|x\|_r \leq \|x\|_s$ for $s \leq r$, we conclude with $r = 2(q-p)/p \geq 2$

$$\|\mathcal{N}'_{p,q}(x_n)\|_2^2 = \left(\frac{q}{p}\right)^2 \|x_n\|_r^r \leq \left(\frac{q}{p}\right)^2 \|x_n\|_2^r \leq C, \tag{4.7}$$

because weakly convergent sequences are uniformly bounded. Thus we obtain

$$\mathcal{N}'_{p,q}(x_n) \rightharpoonup \mathcal{N}'_{p,q}(x).$$

With the same arguments, we find for a fixed z

$$\mathcal{N}'_{p,q}(x_n)z \rightharpoonup \mathcal{N}'_{p,q}(x)z.$$

The convergence of this sequence holds also in the strong sense. For this, it is sufficient to show that $\lim_{n\to\infty} \|\mathcal{N}'_{p,q}(x_n)z\| = \|\mathcal{N}'_{p,q}(x)z\|$ holds. As x_n is weakly convergent, it is also uniformly bounded, i.e., $\|x_n\|_{\ell_2} \leq \tilde{C}$. Thus the components of this sequence are uniformly bounded, $|x_{n,k}| \leq \tilde{C}$, yielding $|x_{n,k}|^{2(q-p)/p} \cdot z_k^2 \leq \tilde{C}^{2(q-p)/p} z_k^2$. We observe that

$$\left(\frac{q}{p}\right)^2 \sum_k |x_{n,k}|^{\frac{2(q-p)}{p}} \cdot z_k^2 \leq \left(\frac{q}{p}\right)^2 \tilde{C}^{\frac{2(q-p)}{p}} \sum_k z_k^2 = \left(\frac{q}{p}\right)^2 \tilde{C}^{\frac{2(q-p)}{p}} \|z\|_2^2 < \infty.$$

Therefore, by the dominated convergence theorem, we can interchange limit and summation, i.e.,

$$\begin{aligned}
\lim_{n\to\infty} \|\mathcal{N}'_{p,q}(x_n)z\|_2^2 &= \lim_{n\to\infty} \left(\frac{q}{p}\right)^2 \sum_k |x_{n,k}|^{2(q-p)/p} \cdot z_k^2 \\
&= \left(\frac{q}{p}\right)^2 \sum_k \lim_{n\to\infty} |x_{n,k}|^{2(q-p)/p} \cdot z_k^2 \\
&= \left(\frac{q}{p}\right)^2 \sum_k |x_k|^{2(q-p)/p} \cdot z_k^2 = \left(\frac{q}{p}\right)^2 \|\mathcal{N}'_{p,q}(x)z\|_2^2,
\end{aligned}$$

and thus

$$\mathcal{N}'_{p,q}(x_n)z \xrightarrow{\ell_2} \mathcal{N}'_{p,q}(x)z. \tag{4.8}$$

We further conclude that

$$\begin{aligned}
&\| ((\mathcal{F}\circ\mathcal{N}_{p,q})'(x_n))^* z - ((\mathcal{F}\circ\mathcal{N}_{p,q})'(x))^* z\|_2 \\
&\quad = \|\mathcal{N}'_{p,q}(x_n)\mathcal{F}'(\mathcal{N}_{p,q}(x_n))^* z - \mathcal{N}'_{p,q}(x)\mathcal{F}'(\mathcal{N}_{p,q}(x))^* z\|_2 \\
&\quad \leq \underbrace{\|\mathcal{N}'_{p,q}(x_n)\mathcal{F}'(\mathcal{N}_{p,q}(x_n))^* z - \mathcal{N}'_{p,q}(x_n)\mathcal{F}'(\mathcal{N}_{p,q}(x))^* z\|_2}_{D_1} \\
&\qquad\quad + \underbrace{\|\mathcal{N}'_{p,q}(x_n)\mathcal{F}'(\mathcal{N}_{p,q}(x))^* z - \mathcal{N}'_{p,q}(x)\mathcal{F}'(\mathcal{N}_{p,q}(x))^* z\|_2}_{D_2},
\end{aligned}$$

and by Proposition 3.2 we obtain

$$\mathcal{N}_{p,q}(x_n) \overset{\ell_2}{\rightharpoonup} \mathcal{N}_{p,q}(x). \tag{4.9}$$

Hence, the two terms can be estimated as follows:

$$D_1 \leq \underbrace{\|\mathcal{N}'_{p,q}(x_n)\|_2}_{\overset{(4.7)}{\leq} C} \underbrace{\| \mathcal{F}'(\mathcal{N}_{p,q}(x_n))^* z - \mathcal{F}'(\mathcal{N}_{p,q}(x))^* z\|_2}_{\xrightarrow{(4.6),(4.9)} 0}$$

and therefore $D_1 \to 0$. For D_2 we obtain with $\tilde{z} := \mathcal{F}'(\mathcal{N}_{p,q}(x))^* z$

$$D_2 = \|\mathcal{N}'_{p,q}(x_n)\tilde{z} - \mathcal{N}'_{p,q}(x)\tilde{z}\|_2 \xrightarrow{(4.8)} 0,$$

which concludes the proof. ☐

In the final step of this section we show the Lipschitz continuity of the derivative.

PROPOSITION 4.5. *Assume that $\mathcal{F}'(x)$ is (locally) Lipschitz continuous with constant L. Then $(\mathcal{F}\circ\mathcal{N}_{p,q})'(x)$ is locally Lipschitz for $p < 1$ and $1 \leq q \leq 2$ such that $2p < q$.*

Proof. The function $f(t) = |t|^s$ with $s > 1$ is locally Lipschitz continuous, i.e., we have on a bounded interval $[a, b]$:

$$|f(t) - f(\tilde{t})| \leq s \max_{\tau\in[a,b]} |\tau|^{s-1}|t - \tilde{t}|. \tag{4.10}$$

Assume $x \in B_\rho(x_0)$, then $\|x\|_2 \leq \|x - x_0\|_2 + \|x_0\|_2 \leq \rho + \|x_0\|_2$ and therefore

$$\sup_{x\in B_\rho(0)} \|x\|_2 \leq \rho + \|x_0\|_2 =: \tilde{\rho}.$$

We have that $s := (q - p)/p \geq 1$, and $|t|^s$ is locally Lipschitz according to (4.10). $\mathcal{N}'_{p,q}(x)$ is a diagonal matrix, thus we obtain with Lemma 4.3 for $x, \tilde{x} \in B_\rho(x_0)$

$$\begin{aligned}
\|\mathcal{N}'_{p,q}(x) - \mathcal{N}'_{p,q}(\tilde{x})\|^2 &= \left(\frac{q}{p}\right)^2 \sum_k \left(|x_k|^{(q-p)/p} - |\tilde{x}_k|^{(q-p)/p}\right)^2 \\
&\overset{(4.10)}{\leq} \left(\frac{q}{p}\right)^2 \left(\frac{q-p}{p}\tilde{\rho}^{(q-2p)/p}\right)^2 \sum_k |x_k - \tilde{x}_k|^2 \\
&\leq \left(\frac{q}{p}\right)^2 \left(\frac{q-p}{p}\tilde{\rho}^{(q-2p)/p}\right)^2 \|x - \tilde{x}\|_2^2.
\end{aligned}$$

With the same arguments, we show that $\mathcal{N}_{p,q}$ is Lipschitz,

$$\|\mathcal{N}_{p,q}(x) - \mathcal{N}_{p,q}(\tilde{x})\|_2 \leq \frac{q}{p}\tilde{\rho}^{(q-p)/p}\|x - \tilde{x}\|_2.$$

The assertion now follows from

$$\begin{aligned}
&\|\mathcal{F}'(\mathcal{N}_{p,q}(x))\mathcal{N}'_{p,q}(x) - \mathcal{F}'(\mathcal{N}_{p,q}(\tilde{x}))\mathcal{N}'_{p,q}(\tilde{x})\| \\
&\qquad \leq \|\left(\mathcal{F}'(\mathcal{N}_{p,q}(x)) - \mathcal{F}'(\mathcal{N}_{p,q}(\tilde{x}))\right)\mathcal{N}'_{p,q}(x)\| \\
&\qquad\qquad + \|\mathcal{F}'(\mathcal{N}_{p,q}(\tilde{x}))\left(\mathcal{N}'_{p,q}(x) - \mathcal{N}'_{p,q}(\tilde{x})\right)\| \\
&\qquad \leq L\|\mathcal{N}_{p,q}(x) - \mathcal{N}_{p,q}(\tilde{x})\|\|\mathcal{N}'_{p,q}(x)\| \\
&\qquad\qquad + \|\mathcal{F}'(\mathcal{N}'_{p,q}(\tilde{x}))\|\|\mathcal{N}'_{p,q}(x) - \mathcal{N}'_{p,q}(\tilde{x})\| \\
&\qquad \leq \tilde{L}\|x - \tilde{x}\|,
\end{aligned}$$

with

$$\tilde{L} = L \max_{x\in B_\rho}\|\mathcal{N}'_{p,q}(x)\|\,\frac{q}{p}\,\tilde{\rho}^{(q-p)/p} + \max_{x\in B_\rho}\|\mathcal{F}'(\mathcal{N}_{p,q}(x))\|\left(\frac{q}{p}\right)^2\frac{q-p}{p}\tilde{\rho}^{(q-2p)/p}. \qquad \square$$

Combining the results of Lemma 4.2 and Propositions 4.1, 4.4, and 4.5, we obtain

PROPOSITION 4.6. *Let $0 < p < 1$ and choose $1 < q \leq 2$ such that $2p < q$. Let $x_n \rightharpoonup x$ with respect to the topology on ℓ_2 and $y \in \ell_2$. Assume that the operator $\mathcal{F} : \ell_2 \to \ell_2$ is Fréchet differentiable and fulfills conditions* (4.1)–(4.3). *Then $\mathcal{G} = \mathcal{F} \circ \mathcal{N}_{p,q}$ is also Fréchet differentiable and we have that for any bounded set $\Omega \subseteq D(\mathcal{F})$, there exists an $L > 0$ such that*

$$\mathcal{G}(x_n) \to \mathcal{G}(x) \quad \text{for } n \to \infty, \tag{4.11}$$

$$\mathcal{G}'(x_n)^* y \to \mathcal{G}'(x)^* y \quad \text{for } n \to \infty, \tag{4.12}$$

$$\|\mathcal{G}'(x) - \mathcal{G}'(x')\|_2 \leq L\,\|x - x'\|_2 \quad \text{for } x, x' \in \Omega. \tag{4.13}$$

Proof. Proposition 4.1 yields (4.11). According to Lemma 4.2, $\mathcal{G}$ is differentiable. By the hypothesis $q > 2p$, the conditions of Proposition 4.4 and Proposition 4.5 hold and thus also (4.12) and (4.13), respectively. $\square$

5. Minimization by surrogate functionals. In order to compute a minimizer of the Tikhonov functional (1.2), we can either use algorithms that minimize (1.2) directly, or alternatively, we can try to minimize (2.1). It turns out that the transformed functional with an ℓ_q-norm and $q > 1$ as penalty can be minimized more effectively by the proposed or other standard algorithms. The main drawback of the transformed functional is that, due to the transformation, we have to deal with a nonlinear operator even if the original operator $\mathcal{F}$ is linear.

A well investigated algorithm for the minimization of the Tikhonov functional with an ℓ_q-penalty that works for all $1 \leq q \leq 2$ is the minimization via surrogate functionals. The method was introduced by Daubechies, Defrise, and De Mol [15] for penalties with $q \geq 1$ and linear operators $\mathcal{F}$. Later on, the method was generalized in [37, 39, 40] to nonlinear operators $\mathcal{G} = \mathcal{F} \circ \mathcal{N}_{p,q}$. The method works as follows: for a given iterate x^n, we consider the surrogate functional

$$\tilde{J}^s_\alpha(x, x^n) = \begin{cases} \|y^\delta - \mathcal{G}(x)\|^2 + \alpha\|x\|_q^q & \\ \qquad + C\|x - x^n\|_2^2 - \|\mathcal{G}(x) - \mathcal{G}(x^n)\|_2^2 & x \in D(\mathcal{G}), \\ +\infty & \text{else,} \end{cases} \tag{5.1}$$

and determine the new iterate as

$$x^{n+1} = \operatorname*{argmin}_x \tilde{J}^s_\alpha(x, x^n). \tag{5.2}$$

The constant C in the definition of the surrogate functional has to be chosen large enough; for more details see [37, 39]. Now it turns out that the functional $\tilde{J}^s_\alpha(x, x^n)$ can be easily minimized by means of a fixed point iteration. For fixed x^n, the functional is minimized by the limit of the fixed point iteration

$$x^{n,l+1} = \Phi_q^{-1}\left(\frac{1}{C}\mathcal{G}'(x^{n,l})^*\left(y^\delta - \mathcal{G}(x^n)\right) + x^n\right), \tag{5.3}$$

where $x^{n,0} = x^n$ and $x^{n+1} = \lim_{l\to\infty} x^{n,l}$. For $q > 1$, the map Φ_q is defined componentwise for an element in a sequence space as

$$\Phi_q(x) = \Phi_q(\{x\}_k) = \{\Phi_q(x_k)\}_k\,,$$
$$\Phi_q(x_k) = x_k + \frac{\alpha \cdot q}{C}|x_k|^{q-1}\operatorname{sgn}(x_k).$$

Thus, in order to compute the new iterate $x^{n,l+1}$, we have to solve the equation

$$\Phi_q\left(\{x^{n,l+1}\}_k\right) = \left\{\frac{1}{C}\mathcal{G}'(x^{n,l})^*\left(y^\delta - \mathcal{G}(x^n)\right) + x^n\right\}_{k\in\mathbb{N}} \tag{5.4}$$

for each $k \in \mathbb{N}$. It has been shown that the fixed point iteration converges to the unique minimizer of the surrogate functional $\tilde{J}^s_\alpha(x, x^n)$ provided the constant C is chosen large enough and the operator fulfills the requirements (4.1)–(4.3); for full details we refer the reader to [37, 39]. Moreover, it has also been shown that the outer iteration (5.2) converges at least to a critical point of the Tikhonov functional

$$\tilde{J}_{\alpha,q}(x) = \begin{cases} \|y^\delta - \mathcal{G}(x)\|_2^2 + \alpha\|x\|_q^q & x \in D(\mathcal{G}), \\ +\infty & \text{else,} \end{cases}$$

provided that the operator $\mathcal{G}$ fulfills the conditions (4.11)–(4.13).

Based on the results of Section 2, we can now formulate our main result.

THEOREM 5.1. *Let $\mathcal{F} : \ell_2 \to \ell_2$ be a weakly (sequentially) closed operator fulfilling the conditions (4.1)–(4.3), and choose $q > 1$ such that $2p < q$, with $0 < p < 1$. Then the operator $\mathcal{G}(x) = \mathcal{F} \circ \mathcal{N}_{p,q}$ is Fréchet differentiable and fulfills the conditions (4.11)–(4.13).*

The iterates x_n computed by the surrogate functional algorithm (5.2) converge at least to a critical point of the functional

$$\tilde{J}_{\alpha,q}(x) = \begin{cases} \|y^\delta - \mathcal{G}(x)\|_2^2 + \alpha\|x\|_q^q & x \in D(\mathcal{G}), \\ +\infty & \textit{else.} \end{cases} \tag{5.5}$$

If the limit of the iteration $x_\alpha^\delta := \lim_{n\to\infty} x^n$ is a global (local) minimizer of (5.5), then $x^\delta_{s,\alpha} := \mathcal{N}_{p,q}(x^\delta_\alpha)$ is a global (local) minimizer of

$$J_{\alpha,p}(x_s) = \begin{cases} \|y^\delta - \mathcal{F}(x_s)\|_2^2 + \alpha\|x_s\|_p^p & x_s \in D(\mathcal{F}), \\ +\infty & \textit{else.} \end{cases} \tag{5.6}$$

Proof. According to Proposition 4.6, the operator $\mathcal{G}$ fulfills the properties that are sufficient for the convergence of the iterates to a critical point of the Tikhonov functional (5.5); see [37, Proposition 4.7]. If x_α^δ is a global minimizer of (5.5), then, according to Proposition 2.6, $x_{s,\alpha}^\delta$ is a minimizer of (1.2). Let x_α^δ be local minimizer. Then there exists a neighborhood $U_\epsilon\left(x_\alpha^\delta\right)$ such that

$$\forall x \in U_\epsilon\left(x_\alpha^\delta\right): \quad \left\|y^\delta - \mathcal{G}(x)\right\|_{\ell_2}^2 + \alpha\left\|x\right\|_q^q \geq \left\|y^\delta - \mathcal{G}\left(x_\alpha^\delta\right)\right\|_{\ell_2}^2 + \alpha\left\|x_\alpha^\delta\right\|_q^q .$$

Let $M := \{x_s : \mathcal{N}_{p,q}^{-1}(x_s) \in U_\epsilon\left(x_\alpha^\delta\right)\}$ and $x_{s,\alpha}^\delta := \mathcal{N}_{p,q}\left(x_\alpha^\delta\right)$, then we can derive that

$$\forall x_s \in M: \quad \left\|y^\delta - \mathcal{F}(x_s)\right\|_{\ell_2}^2 + \alpha\left\|x_s\right\|_p^p \geq \left\|y^\delta - \mathcal{F}\left(x_{s,\alpha}^\delta\right)\right\|_{\ell_2}^2 + \alpha\left\|x_{s,\alpha}^\delta\right\|_p^p .$$

Since $\mathcal{N}_{p,q}$ and $\mathcal{N}_{p,q}^{-1}$ are continuous, there exists a neighborhood U_{ϵ_s} around the solution of the original functional $x_{s,\alpha}^\delta$ such that $U_{\epsilon_s}(x_{s,\alpha}^\delta) \subseteq M$. □

Theorem 5.1 is based on the transformed functional. Whenever a global or local minimizer is reconstructed, the result can be directly interpreted in terms of the original functional (5.6). As it can be seen from the proof, this can be generalized to stationary points. Assuming that the limit of the iteration is no saddle point, any stationary point of the transformed functional is also a stationary point of (5.6).

Concerning the iterative scheme (5.3), the question arises which impact the introduced transformation operator has. Below we discuss these effects in the light of the shrinkage operator Φ_q^{-1}. Let x denote the current inner iterate $x^{(n,l)}$ and s the fixed current outer iterate $x^{(n)}$, then one iteration step of the above scheme is given by

$$\begin{aligned}
&\Phi_q^{-1}\left(\frac{1}{C}\mathcal{G}'\left(x\right)^*\left(y^\delta - \mathcal{G}\left(s\right)\right) + s\right)\\
&\qquad = \Phi_q^{-1}\left(\frac{1}{C}\mathcal{N}_{p,q}'(x)\mathcal{F}'\left(\mathcal{N}_{p,q}(x)\right)^*\left(y^\delta - \mathcal{F}\left(\mathcal{N}_{p,q}(s)\right)\right) + s\right)\\
&\qquad = \Phi_q^{-1}\left(\mathcal{N}_{p,q}'(x)\left(\frac{1}{C}\mathcal{F}'\left(\mathcal{N}_{p,q}(x)\right)^*\left(y^\delta - \mathcal{F}\left(\mathcal{N}_{p,q}(s)\right)\right) + \mathcal{N}_{p,q}'(x)^{-1}s\right)\right).
\end{aligned} \tag{5.7}$$

In (5.7), the transformation operator occurs several times. One instance is $\mathcal{F}(\mathcal{N}_{p,q}(s))$. Bearing in mind that we apply the iterative scheme on the transformed functional (5.5) and that consequently $s \in \ell_q$, the role of $\mathcal{N}_{p,q}$ is to map s to the domain of $\mathcal{F}$, which is defined with respect to ℓ_p. The same observation applies to the term $\mathcal{F}'\left(\mathcal{N}_{p,q}(x)\right)^*$.

The next term which is influenced by the transformation operator in the iteration (5.7) is $\mathcal{N}_{p,q}'(x)^{-1}s$. The additive term can be interpreted as an offset for the shrinkage operation and restricts large changes in each iteration. Note that this term arises due to the stabilizing term in the surrogate functional having exactly the purpose of penalizing large steps. However, in our approach we apply the surrogate technique on the transformed problem (5.5) and thus penalize the step size with respect to the transformed quantities. Hence, the respective term in the update formula (5.3) is independent of the transformation operator, which leads to the term $\mathcal{N}_{p,q}'(x)^{-1}s$ in the above formulation (5.7), where we singled out the linear operator $\mathcal{N}_{p,q}'(x)$. Accordingly, we have that the entire argument of the shrinkage operator Φ_q^{-1} is scaled by $\mathcal{N}_{p,q}'(x)$ leading to the map $t \mapsto \Phi_q^{-1}\left(\mathcal{N}_{p,q}'(x)t\right)$. This can be regarded as the main impact of the transformation strategy on the iterative thresholding algorithm. In that regard, we are interested in fixed points with respect to x, i.e.,

$$t \mapsto x^* \quad \text{where} \quad x^* = \Phi_q^{-1}\left(\mathcal{N}_{p,q}'(x^*)t\right), \tag{5.8}$$

which corresponds to the fixed point iteration in (5.3).

Figure 5.1 shows the value of the fixed point equation $x^* = \Phi_q^{-1}\left(\mathcal{N}'_{p,q}(x^*)t\right)$ in dependence of t. The solid line refers to the case of $p = 0.9$ and the dashed one to the case of $p = 0.8$. In both case, q is chosen to be 1.2. We observe a behavior of the map (5.8) close to that of the so-called hard- or firm thresholding. Moreover, the plot in Figure 5.1 shows that for an increasing value of p, the map (5.8) approaches the standard thresholding function; see also Figure 5.2. On the other hand, decreasing values of p lead to a more pronounced thresholding and particularly to a discontinuous separation between values of t which are clipped and which are increased by trend, i.e., are subject to hard thresholding.

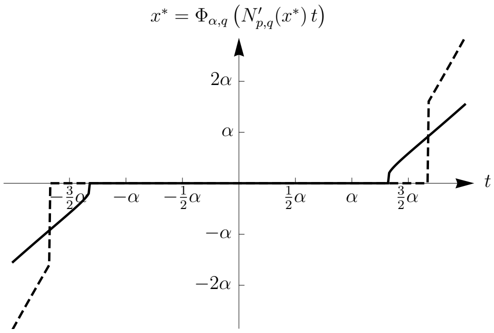

FIGURE 5.1. *One-dimensional outline of the relation between the fixed point of the map* $x \mapsto \Phi_q^{-1}\left(\mathcal{N}'_{p,q}(x)t\right)$ *and the value of* t *for* $p = 0.9$ *(solid line),* $p = 0.8$ *(dashed line), and* $q = 1.2$*. A smaller value of* p *leads to a pronounced hard thresholding and an increased range of thresholding. Moreover the slope outside the range of thresholding is increased.*

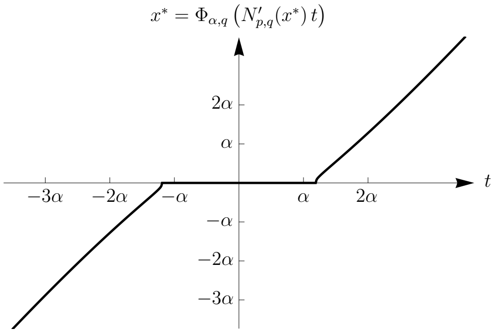

FIGURE 5.2. *One-dimensional outline of the map* (5.8) *for* $p = 0.95$ *(*$q = 1.2$*) and a larger scale of* t*-values (compared to the previous plots). The map exhibits a behavior similar to the thresholding function.*

Note that the thresholding as represented by our map (5.8) crucially depends on the respective value of the current iterate. In particular, the implication of the superposition operator allows for an increased or decreased (i.e., adaptive) range of thresholding depending on the magnitude of the current iterate x (denoted by $x^{(n,l)}$ in (5.3)). Figure 5.3 displays this scenario for the case of $p = 0.8$ and $q = 1.2$. Let x_0^* denote the initial guess for the fixed point map, which is the current iterate of the outer loop, i.e., $x^{(n)}$ in (5.3). The dotted line in Figure 5.3 shows the case of $x_0^* = 10$, the dashed line the case of $x_0^* = 0.1$, and the solid line the choice of $x_0^* = 0.05$. Note that for all previous plots on that matter we always chose $x_0^* = 1$ to ensure comparable results. The increase of the range of thresholding for decreasing values of $x^{(n)}$ leads to a strong promotion of zero values and thus to presumably

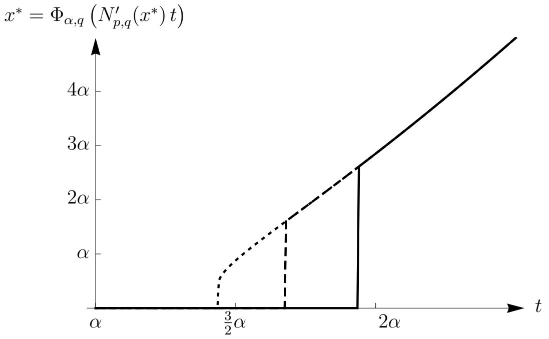

FIGURE 5.3. *One-dimensional outline of the map (5.8) for $p = 0.8$ and $q = 1.2$ for different initial values x_0^* for the fixed point iteration (dotted line: $x_0^* = 10$, dashed line: $x_0^* = 0.1$, solid line: $x_0^* = 0.05$). For decreasing values of the initial values the range of thresholding is increased.*

sparse solutions.

We conclude that the transformation operator acts as an adaptive scaling of the shrinkage operator depending on the respective values of the current inner iterates. The basic effect of this scaling is that the fixed point map (5.8) exhibits a behavior similar to hard thresholding, where smaller values of p enhance this effect. Moreover, the values of the current iterates are crucial for the range of thresholding and lead to an adaptive behavior. In particular, thresholding is enhanced for small x and reduced for large x. This matches the idea of promoting sparse solutions by penalizing small components increasingly and hardly penalizing large components.

6. A global minimization strategy for the transformed Tikhonov functional: the case $q = 2$**.** The minimization by surrogate functionals presented in Section 5 guarantees the reconstruction of a critical point of the transformed functional only. If we have not found the global minimizer of the transformed functional, then this also implies that we have not reconstructed the global minimizer for the original functional. In this section we would like to recall an algorithm that, under some restrictions, guarantees the reconstruction of a global minimizer. In contrast to the surrogate functional approach, this algorithm works in the case of $q = 2$ only, i.e., we are looking for a global minimizer of the standard Tikhonov functional

$$\tilde{J}_{\alpha,2}(x) = \begin{cases} \|y^\delta - \mathcal{G}(x)\|^2 + \alpha\|x\|_2^2 & x_s \in D(\mathcal{G}), \\ +\infty & \text{else} \end{cases} \tag{6.1}$$

with $\mathcal{G}(x) = \mathcal{F}(\mathcal{N}_{p,2}(x))$. For the minimization of the functional, we want to use the TIGRA method [35, 36]. The main ingredient of the algorithm is a standard gradient method for the minimization of (6.1), i.e., the iteration is given by

$$x^{n+1} = x^n + \beta_n \left(\mathcal{G}'(x^n)^*(y^\delta - \mathcal{G}(x^n)) - \alpha x^n\right). \tag{6.2}$$

The following arguments are taken out of [36], where the reader finds all the proofs and further details. If the operator $\mathcal{G}$ is twice Fréchet differentiable, its first derivative is Lipschitz continuous, and a solution $x^\dagger$ of $\mathcal{G}(x) = y$ fulfills the smoothness condition

$$x^\dagger = \mathcal{G}'(x^\dagger)^*\omega, \tag{6.3}$$

then it has been shown that (6.1) is locally convex around a global minimizer x_α^δ. If an initial guess x^0 within the area of convexity is known, then the scaling parameter β_n can be chosen such that all iterates stay within the area of convexity and $x^n \to x_\alpha^\delta$ as $n \to \infty$. However, the area of convexity shrinks to zero if $\alpha \to 0$, i.e., a very good initial guess for smaller α is needed. For an arbitrary initial guess x^0, this problem can be overcome by choosing a monotonically decreasing sequence $\alpha_0 > \alpha_1 > \cdots > \alpha_n = \alpha$ with sufficiently large α_0 and a small step size α_{i+1}/α_i, and then iterate as follows:

```
Input: $x^0, \alpha_0, \cdots, \alpha_n$
Iterate: For $i = 1, \cdots, n$
    • If $i > 1$, set $x^0 = x^\delta_{\alpha_{i-1}}$.
    • Minimize $\tilde{J}_{\alpha_i,2}(x)$ by the gradient method (6.2) and initial value $x^0$.
End
```

We wish to remark that the iteratively regularized Landweber iteration, introduced by Scherzer [43], is closely related to TIGRA. Its iteration is similar to (6.2) but requires the use of a summable sequence α_k (instead of a fixed α). In contrast to TIGRA, the iteratively regularized Landweber iteration aims at the solution of a nonlinear equation and not on the minimization of a Tikhonov functional. Additionally, the iteratively regularized Landweber iteration requires more restrictive conditions on the nonlinear operator.

In a numerical realization, the iteration (6.2) has to be stopped after finitely many steps. Therefore the final iterate is taken as starting value for the minimization of the Tikhonov functional with the next regularization parameter. As mentioned above, this procedure reconstructs a global minimizer of $J_{\alpha,p}$ if the operator $\mathcal{G}$ is twice Fréchet differentiable, its first derivative is Lipschitz continuous, and (6.3) holds [36]. We will verify these conditions for two important cases, namely when $\mathcal{F}$ is the identity (i.e., the problem of data denoising) and when $\mathcal{F}$ is a linear operator, $\mathcal{F} = \mathcal{A}$.

PROPOSITION 6.1. *The operator $\mathcal{N}_{p,2}(x)$, with $0 < p < 1$, is twice continuously differentiable and therefore also the operator $\mathcal{A}\mathcal{N}_{p,2}(x)$ with a continuous and linear $\mathcal{A}$.*

Proof. The proof is completely analogous to the one of Proposition 3.5 considering the fact that $\frac{2}{p} \geq 2$. Using the Taylor expansion of the function $\eta_{p,2}(t) = |t|^{2/p}\,\mathrm{sgn}(t)$

$$\eta_{p,2}(t+\tau) - \eta_{p,2}(t) - \eta'_{p,2}(t)\tau - \frac{1}{2}\eta''_{p,2}(t)\tau^2 := r(t,\tau),$$

with

$$\eta''{}_{p,2}(t) = \frac{2(2-p)}{p^2}\,\mathrm{sgn}(t)|t|^{2(1-p)/p},$$

one obtains the following representation of the remainder

$$r(t,\tau) = \int_t^{t+\tau} \frac{1}{2}\frac{2}{p}\frac{2-p}{p}\frac{2-2p}{p}(t+\tau-s)^2|s|^{\frac{2}{p}-3}\,\mathrm{d}s.$$

Again by the mean value theorem and using Lemma 3.3 with $\alpha = \frac{2}{p} - 2$, we obtain

$$\begin{aligned}
&\left|\int_t^{t+\tau} \frac{1}{2}\frac{2}{p}\frac{2-p}{p}\frac{2-2p}{p}(t+\tau-s)^2|s|^{\frac{2}{p}-3}\,\mathrm{d}s\right| = \\
&= \left|\left[\frac{1}{2}\frac{2}{p}\frac{2-p}{p}(t+\tau-s)^2|s|^{\frac{2}{p}-2}\right]_t^{t+\tau} + \int_t^{t+\tau}\frac{2}{p}\frac{2-p}{p}(t+\tau-s)|s|^{\frac{2}{p}-2}\,\mathrm{d}s\right| \\
&= \left|\tau\frac{2}{p}\frac{2-p}{p}\left((t+\tau-\xi)\,\mathrm{sgn}(\xi)|\xi|^{2/p-2} - \frac{1}{2}\tau\,\mathrm{sgn}(t)|t|^{2/p-2}\right)\right| \\
&\overset{(3.1)}{\leq} \tilde{\kappa}\frac{2}{p}\frac{2-p}{p}|\tau|^{w+2},
\end{aligned}$$

where $\xi \in (t, t+\tau)$, $w := \min\left(\frac{2}{p} - 2, 1\right) > 0$. One may notice that the scaling factor $1/2$ requires a redefinition of κ in Lemma 3.3 leading to $\tilde{\kappa}$. Eventually, we conclude that

$$\left\| \mathcal{N}'_{p,2}(x+h)\bar{h} - \mathcal{N}'_{p,2}(x)\bar{h} - \mathcal{N}''_{p,2}(x)(\bar{h}, h) \right\|_2 / \left\| h \right\|_2 \to 0 \quad \text{for } \left\| h \right\|_2 \to 0$$

analogously to the proof of Proposition 3.5. Thus we have

$$\mathcal{N}''_{p,2}(x)(\bar{h}, h) = \left\{ \eta''_{p,q}(x_k)\bar{h}_k h_k \right\}_{k \in \mathbb{N}}.$$

The twice differentiability of $\mathcal{A}\mathcal{N}_{p,2}(x)$ follows from the linearity of $\mathcal{A}$. □

Now let us turn to the source condition (6.3).

PROPOSITION 6.2. *Let* $\mathcal{F} = \mathcal{I}$. *Then* $x^\dagger \in \ell_2$ *fulfills the source condition* (6.3) *if and only if it is sparse, i.e., it has only finitely many nonzero coefficients.*

Proof. As $\mathcal{I} = \mathcal{I}^*$ in ℓ_2, we have $\mathcal{F}'(\mathcal{N}_{p,2}(x^\dagger))^* = \mathcal{I}$, and it follows from (4.5) that

$$\left(\mathcal{F}(\mathcal{N}_{p,2}(x))'\right)^* = \mathcal{N}'_{p,2}(x).$$

Therefore, the source condition (6.3) reads coefficient-wise as

$$\frac{2}{p}|x_k^\dagger|^{(2-p)/p}\omega_k = x_k^\dagger$$

or

$$\omega_k = \frac{2}{p}\,\mathrm{sgn}(x_k^\dagger)|x_k^\dagger|^{(2p-2)/p},$$

for $x_k \neq 0$. For $x_k = 0$, we can set $w_k = 0$, too. As $\omega_k,\ x^\dagger \in \ell_2$, and $2p - 2 < 0$, this can only hold if $x^\dagger$ has only a finite number of nonzero elements. □

The case of $\mathcal{F} = \mathcal{A}$ is a little bit more complicated. In particular, we require the operator $\mathcal{A}$ to fulfill the finite basis injectivity (FBI) property which was introduced by Bredies and Lorenz [7]. Let $\mathcal{T}$ be a finite index set, and let $\#\mathcal{T}$ be the number of elements in $\mathcal{T}$. We say that $u \in \ell_2(\mathcal{T})$ if and only if $u_k = 0$ for all $k \in \mathbb{N} \setminus \mathcal{T}$. The FBI property states that whenever $u, v \in \ell_2(\mathcal{T})$ with $\mathcal{A}u = \mathcal{A}v$, it follows that $u = v$. This is equivalent to

$$\mathcal{A}_{|\ell_2(\mathcal{T})} u = 0 \Longrightarrow u = 0,$$

where $\mathcal{A}_{|\ell_2(\mathcal{T})}$ is the restriction of $\mathcal{A}$ to $\ell_2(\mathcal{T})$. For simplicity we set $\mathcal{A}_{|\ell_2(\mathcal{T})} = \mathcal{A}_\mathcal{T}$.

PROPOSITION 6.3. *Assume that* $x^\dagger$ *is sparse,* $\mathcal{T} = \{k : x_k^\dagger \neq 0\}$, *and that* $\mathcal{A} : \ell_2 \to \ell_2$ *is bounded. If* $\mathcal{A}$ *has the FBI property, then* $x^\dagger$ *fulfills the source condition* (6.3).

Proof. As $x^\dagger$ is sparse, $\mathcal{T}$ is finite. By $x_\mathcal{T}$ we denote the (finite) vector that contains only those elements of x with indices in $\mathcal{T}$. Because $\mathcal{A}$ is considered being an operator between ℓ_2, we have $\mathcal{A}^* = \mathcal{A}^T$ and $\mathcal{A}_\mathcal{T}^* = \mathcal{A}_\mathcal{T}^T$. Due to the sparse structure of $x^\dagger$, we observe

$$\mathcal{N}'_{p,2}(x^\dagger) : \ell_2 \to \ell_2(\mathcal{T})$$

and therefore also

$$\begin{aligned} \mathcal{A}\mathcal{N}'_{p,2}(x^\dagger) &= \mathcal{A}_\mathcal{T}\mathcal{N}'_{p,2}(x^\dagger) \\ \left(\mathcal{A}\mathcal{N}'_{p,2}(x^\dagger)\right)^* &= \mathcal{N}'_{p,2}(x^\dagger)\mathcal{A}_\mathcal{T}^* = \mathcal{N}'_{p,2}(x^\dagger)\mathcal{A}_\mathcal{T}^T, \end{aligned}$$

where we use the fact that $\mathcal{N}'_{p,2}(x^\dagger)$ is self-adjoint.

With $\mathcal{F} = \mathcal{A}$, (6.3) reads as

$$x^\dagger = \mathcal{N}'_{p,2}(x^\dagger)\mathcal{A}_\mathcal{T}^T\omega.$$

The operator $\mathcal{N}'_{p,2}(x^\dagger)^{-1}$ is well defined on $\ell_2(\mathcal{T})$, and since $\ell_2(\mathcal{T}) = \mathcal{D}(\mathcal{A}_\mathcal{T}) = \mathcal{R}(\mathcal{A}_\mathcal{T}^T)$, we obtain

$$\mathcal{A}_\mathcal{T}^T\omega = \mathcal{N}'_{p,2}(x^\dagger)^{-1}x^\dagger.$$

Now we have by the FBI property $\mathcal{N}(\mathcal{A}_\mathcal{T}) = \{0\}$ and therefore

$$\ell_2(\mathcal{T}) = \mathcal{N}(\mathcal{A}_\mathcal{T})^\perp = \overline{\mathcal{R}(\mathcal{A}_\mathcal{T}^*)} = \overline{\mathcal{R}(\mathcal{A}_\mathcal{T}^T)}.$$

As $\dim(\ell_2(\mathcal{T})) = \#\mathcal{T} < \infty$, $\mathcal{R}(\mathcal{A}_\mathcal{T}^T) = \ell_2(\mathcal{T})$ and therefore the generalized inverse of $\mathcal{A}_\mathcal{T}^T$ exists and is bounded. We finally obtain

$$\omega = \left(\mathcal{A}_\mathcal{T}^T\right)^\dagger \mathcal{N}'_{p,2}(x^\dagger)^{-1}x^\dagger$$

and

$$\|\omega\|_2 \leq \| \left(\mathcal{A}_\mathcal{T}^T\right)^\dagger \|_2 \|\mathcal{N}'_{p,2}(x^\dagger)^{-1}\|_2 \|x^\dagger\|_2. \qquad \square$$

Please note that a similar result can be obtained for twice continuously differentiable nonlinear operators $\mathcal{F}$ if we additionally assume that $\mathcal{F}'(\mathcal{N}_{p,2}(x^\dagger))$ admits the FBI condition. Propositions 6.1–6.3 show that the TIGRA algorithm can in principle be applied to the minimization of the transformed Tikhonov functional for the case $q = 2$ and reconstructs a global minimizer. The surrogate functional approach can also be applied to the case $q < 2$. This is in particular important for the numerical realization, as we show in the following section.

7. Numerical results.

In this section we present some numerical experiments for a deconvolution problem and a parameter identification problem in a mathematical model from physical chemistry. Considering the proposed non-standard approach, we are particularly interested in the impacts of the transformation operator on the numerical realization and the sparsity promoting features of the proposed algorithm.

Beforehand, we address some key points regarding the numerical implementation of the proposed iterative thresholding algorithm. As this approach is based on a Tikhonov-type regularization method, the first crucial issue is the choice of the regularization parameter. To our knowledge there are currently no particular parameter choice rules available explicitly addressing Tikhonov-type methods with non-convex ℓ_p-quasi-norms. However, for the subsequent examples, we design the problems such that we know the solution in advance in order to be able to assess the quality of the reconstruction as well as its sparsity compared to the true solution. Hence, this also allows to accurately determine the regularization parameter. Taking advantage of that fact which we observe for all subsequent numerical examples that the discrepancy principle (cf. [1]) provides rather good estimates of the regularization parameter α, we determine α such that

$$\alpha(\delta, y^\delta) := \sup\left\{\alpha > 0 \ : \ \left\|\mathcal{G}(x_\alpha^\delta) - y^\delta\right\|_{\ell_2} \leq \tau\delta\right\},$$

where x_α^δ is the regularized solution and $\tau > 1$.

The next subject we address is the choice of the surrogate constant C in (5.1). As discussed in [37], the value of C is crucial for the convergence of the algorithm and has to be chosen sufficiently large. However, a large value of C increases the weight on the stabilization term $\|x - s\|_2^2$ in (5.1) and hence decreases the speed of convergence. We propose to use a simple heuristic in order to determine the value of C. We take advantage of the fact that if C is chosen too small, the iteration rapidly diverges, which can be easily detected. In particular, we propose to test the monotone decrease of the surrogate functional and choose C large enough such that the iteration still exhibits the monotonicity. Moreover, we emphasize that C does depend on the norm of the linearized operator G' evaluated at the current iterate. Thus, particularly in the first phase of the iteration, the norm of G' may change significantly. This suggests to adapt the value of C after a few steps in order to increase the speed of convergence.

Another crucial point for the realization of the iterative thresholding scheme (5.3) is the solution of the nonlinear problem (5.4) in the inner iteration, i.e., for each component of the given right-hand side $z \in \mathbb{R}$ (see (5.3)), we seek the corresponding element $x \in \mathbb{R}$ such that

$$z = \Phi_q(x) = x + \frac{\alpha q}{C}|x|^{q-1}\operatorname{sgn}(x)\,. \tag{7.1}$$

For $q < 2$ the nonlinear problem (7.1) is not differentiable and it can be shown that the Newton method fails to converge; cf. [37]. Since (7.1) has to be solved numerous times (in each iteration for every component) throughout the iteration, we propose to use a safeguarded Newton method; cf. [44]. The standard Newton method would fail for x_k close to zero. However, the sign of the solution x_k and the right-hand side z_k coincide and $z_k = 0$ implies $x_k = 0$. Hence, without loss of generality, we can assume $z_k > 0$. This allows to effectively control the step length of the Newton update, in particular we prevent any steps leading to negative values.

7.1. Deconvolution in sequence spaces. Subsequently, we present some numerical results on the reconstruction of a function from convolution data. The example is taken from [38], which we refer to for more details on the problem. We define the convolution operator A by

$$y(\tau) = (Ax)(\tau) = \int_{-\pi}^{\pi} r(\tau - t)x(t)dt =: (r * x)(\tau),$$

where x, r and Au are 2π-periodic functions belonging to $L_2(\Omega)$, with $\Omega = (-\pi, \pi)$. In order to obtain a numerical realization in accordance with the present notation, we identify the occurring quantities with the respective Fourier coefficients. A periodic function on $[-\pi, \pi]$ can be either expressed via the orthonormal bases formed by

$$\left\{\frac{1}{\sqrt{2\pi}}e^{ikt}\right\}_{k\in\mathbb{Z}} \quad \text{or} \quad \left\{\frac{1}{\sqrt{2\pi}}, \frac{1}{\sqrt{\pi}}\cos(kt), \frac{1}{\sqrt{\pi}}\sin(kt)\right\}_{k\in\mathbb{N}}.$$

Using the Fourier convolution theorem for the exponential basis and transformation formulas between the exponential and trigonometrical bases, we obtain an equivalent linear problem in terms of the considered real sequence spaces. Note that due to the nonlinear superposition operator, we still have a nonlinear problem. Consequently, the linear problem serves two purposes. Firstly, a large part of the currently available sparsity promoting algorithms concerns only the case of a linear operator. In particular, also the classical iterative thresholding algorithm has been developed for linear problems. In that regard, a comparison of the performance is interesting. Due to the nonlinear transformation, the question arises whether the problem is artificially complicated or whether the simple structure of the transformation operator nevertheless allows for a compatible performance. We address this issue by comparing our ℓ_p-penalization for $0 < p < 1$ with the classical iterative thresholding technique based on the ℓ_1-norm. Another benefit of the linear problem is that the only nonlinearity in the operator arises due to the superposition operator and thus allows us to study the effects of the nonlinearity due to the transformation technique. Note that concerning the gradient computation, the nonlinear superposition operator poses no disadvantage as its derivative can be computed analytically and implemented efficiently.

For the numerical implementation, we divide the interval $[-\pi, \pi]$ into 2^{12} equidistant intervals leading to a discretization of the convolution operator as a $2^{12} \times 2^{12}$ matrix. We define the convolution kernel r by its Fourier coefficients with

$$a_0^r = 0, \quad a_k^r = (-1)^k \cdot k^{-2}, \quad b_k^r = (-1)^{k+1} \cdot k^{-2},$$

where

$$r(t) = a_0^r + \sum_{k \in \mathbb{N}} a_k^r \cos(kt) + b_k^r \sin(kt). \tag{7.2}$$

The data for the numerical experiments were generated based on a sparse representation of the solution $x^\dagger$ with 14 nonzero components; see Table 7.1. In accordance with (7.2), we may refer to the decomposition of $x^\dagger$ as

$$x^\dagger(t) = a_0^\dagger + \sum_{k \in \mathbb{N}} a_k^\dagger \cos(kt) + b_k^\dagger \sin(kt),$$

where $a^\dagger = \left(x_1^\dagger, \dots, x_{2048}^\dagger\right)$, $a_0^\dagger = x_{2049}^\dagger$, and $b^\dagger = \left(x_{2050}^\dagger, \dots, x_{4097}^\dagger\right)$.

TABLE 7.1

The coefficients of the true solution $x^\dagger$ *with the* 14 *nonzero components are shown, where* $a^{x^\dagger} = \left(x_1^\dagger, \dots, x_{2048}^\dagger\right)$, $a_0^{x^\dagger} = x_{2049}^\dagger$, *and* $b^{x^\dagger} = \left(x_{2050}^\dagger, \dots, x_{4097}^\dagger\right)$ *in accordance with (7.2).*

index	$\left(x_1^\dagger, \dots, x_{2041}^\dagger\right)$			$x_{2042}^\dagger$	$x_{2043}^\dagger$	$x_{2044}^\dagger$	$x_{2045}^\dagger$	$x_{2046}^\dagger$	$x_{2047}^\dagger$	$x_{2048}^\dagger$	$x_{2049}^\dagger$
value	$(0, \dots, 0)$			$\frac{1}{70}$	$\frac{1}{60}$	$\frac{1}{50}$	$\frac{1}{40}$	$\frac{1}{30}$	$\frac{1}{20}$	$\frac{1}{10}$	0
index	$x_{2050}^\dagger$	$x_{2051}^\dagger$	$x_{2052}^\dagger$	$x_{2053}^\dagger$	$x_{2054}^\dagger$	$x_{2055}^\dagger$	$x_{2056}^\dagger$	$\left(x_{2057}^\dagger, \dots, x_{4097}^\dagger\right)$			
value	$-\frac{1}{10}$	$-\frac{1}{20}$	$-\frac{1}{30}$	$-\frac{1}{40}$	$-\frac{1}{50}$	$-\frac{1}{60}$	$-\frac{1}{70}$	$(0, \dots, 0)$			

We perturbed the exact data by a normally distributed noise which was norm-wise (using the $\mathcal{L}_2$-norm) scaled with respect to the data and the noise level, respectively. If not stated otherwise, we use an approximate noise level of five percent relative Gaussian noise.

The first numerical experiment concerns the convergence rate with respect to the noise level. In [45] it was shown that (1.2) provides a regularization method, and a result on rates of convergence was given. The authors prove that under standard assumptions, the convergence of the accuracy error is at least of the order of $\sqrt{\delta}$,

$$\left\| x^* - x_\alpha^\delta \right\|_2 = \mathcal{O}(\sqrt{\delta}).$$

As displayed in Figure 7.1, this rate is even exceeded in our numerical examples, where we observe a linear rate. This is in accordance with recent results on enhanced convergence rates based on the assumption of a sparse solution; cf. [25, 27]. We refer to [46] for a more detailed discussion on this subject.

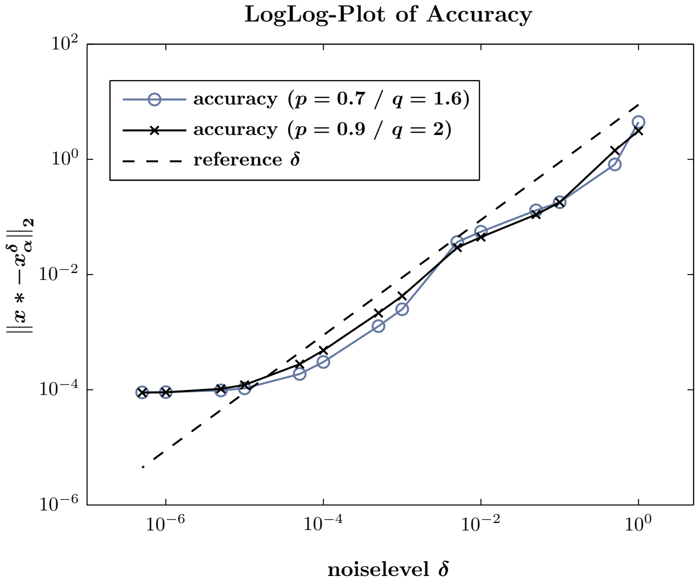

FIGURE 7.1. *The plot shows the numerically observed rate of convergence for the values* $p = 0.9, q = 2$ *and for* $p = 0.7$*,* $q = 1.6$ *compared to the reference rate* δ*.*

Figure 7.1 shows the rates of convergence for decreasing noise levels δ. One may notice that the convergence slows down for very small values of δ. This behavior is well known and can be caused by local minima or too coarse accuracy goals. Another difficulty could be a numerical inaccuracy of the inner iterations (5.3), which might cause a stagnation of the iteration. In fact, the observed loss of accuracy is very pronounced if the error criteria in the inner iteration are not chosen appropriately. This observation seems comprehensible when considering the transformation operator and the fact that all unknowns are raised to a power of q/p. This is also in accordance with our findings of an increased computational effort (a higher iteration number) and the necessity of a sufficiently high numerical precision for decreasingly smaller values of p. These requirements are met by an efficient implementation with stringent error criteria in all internal routines or iterations, respectively. For the inner iteration, we control the absolute error per coefficient

$$\max_k |\{x^{n,l+1} - x^{n,l}\}_k| = \mathcal{O}(10^{-14}),$$

whereas the outer iteration is stopped after a sufficient convergence with respect to the data error and pointwise changes of the parameters is obtained

$$\left\|y^\delta - \mathcal{G}(x^{n+1})\right\|_2^2 = \mathcal{O}(10^{-8}) \quad \text{and} \quad \max_k \left|\{x^{n+1} - x^n\}_k\right| = \mathcal{O}(10^{-6}).$$

Despite the stringent error criterion, the inner loop usually converges within 2 to 10 iterations. The number of outer iterations strongly depends on the respective settings and chosen parameters.

Figure 7.2 shows the exact data curve (without noise) and the obtained reconstructions of the data for various values of p and $q = 2$ and approximately 5% Gaussian noise. The right-hand axis refers to the difference of these curves, which is plotted below. For increasing values of p, the data fit improves. Correspondingly, the number of nonzero coefficients in the reconstructed Fourier coefficients increases as well. For $p = 0.4$, we reconstruct 7 nonzero coefficients, for $p = 0.5$ the obtain solution consists of 7 nonzero components, for $p = 0.7$

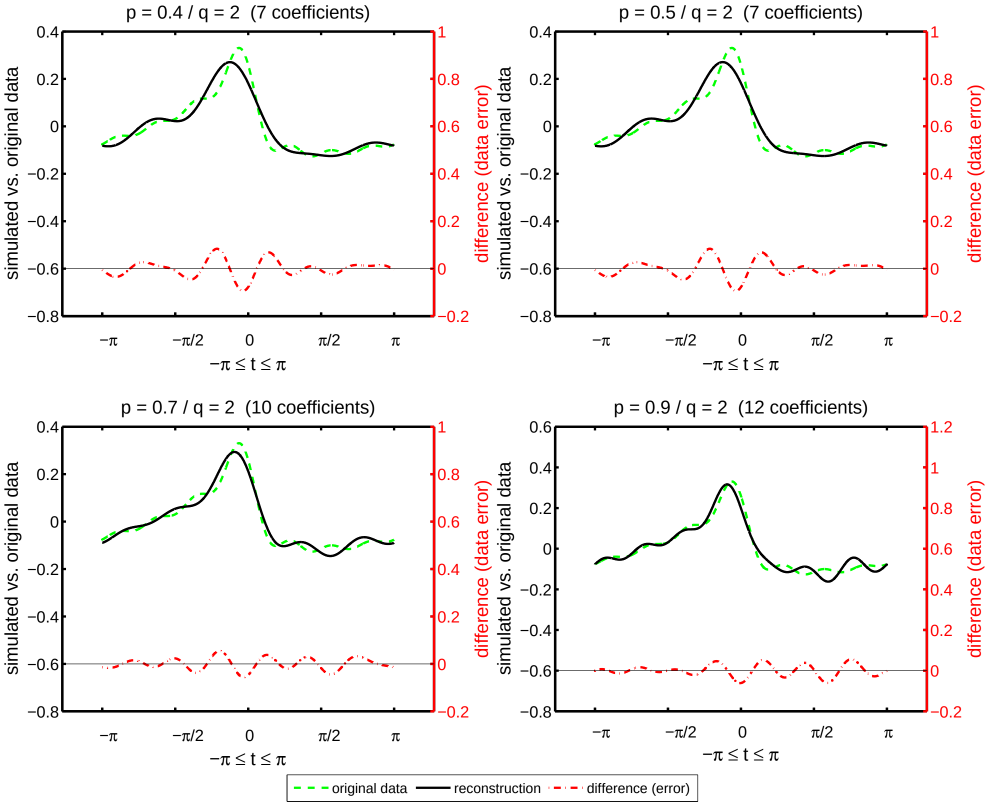

FIGURE 7.2. *The exact data of the deconvolution problem and the obtained simulated data from the reconstructions for* $p = \{0.4, 0.5, 0.7, 0.9\}$ *are plotted. Below, the difference between the (noise free) data curve and the simulated data from the reconstruction is given (see right y-axis).*

we find 10 nonzero coefficients, and for $p = 0.9$ the solution has 12 nonzero coefficients, compared to 14 nonzero entries in the true solution $x^\dagger$. The decreasing number of nonzero coefficients indicates an increased promotion of sparse coefficient vectors for smaller values of p. This is especially worth mentioning since already for $p = 0.9$, the number of nonzero coefficients is underestimated. Furthermore, one may note that the zero components of these solutions are really zero with respect to the machine precision (about 10^{-16}). Only in the solution for $p = 0.9$, $q = 2$, several “outliers” in the order of 10^{-5}–10^{-10} are found. Increasing the error criteria further would provide a remedy.

Additionally, we find that the proposed regularization method is sensitive with respect to the choice of the regularization parameter α, which we account for by using fine grids of values for α ($0.5^{\{0,1,2,\dots,\}}$). Moreover, we would like to emphasize that all the obtained nonzero coefficients are within the support of the true solution $x^\dagger$. Only for $p = 0.9$ and $q = 2$, some of the very small outliers addressed above lie outside the support of the original solution. Eventually, we obtain good data fits for all values of p and q, even in those cases where the reconstructed solution consists only of 4 nonzero components compared to 14 coefficients in the true solution.

Figure 7.3 shows the progress of the iteration routine in the case of $p = 0.7$ and $q = 2$. Due to the high number of unknown coefficients (4097), we consider the progress of the iterates for a sub sample of the coefficients only. After 1500 iterations, all coefficients greater than 10^{-6} lie within the indices 2032 to 2068. The coefficients depicted in the first row are

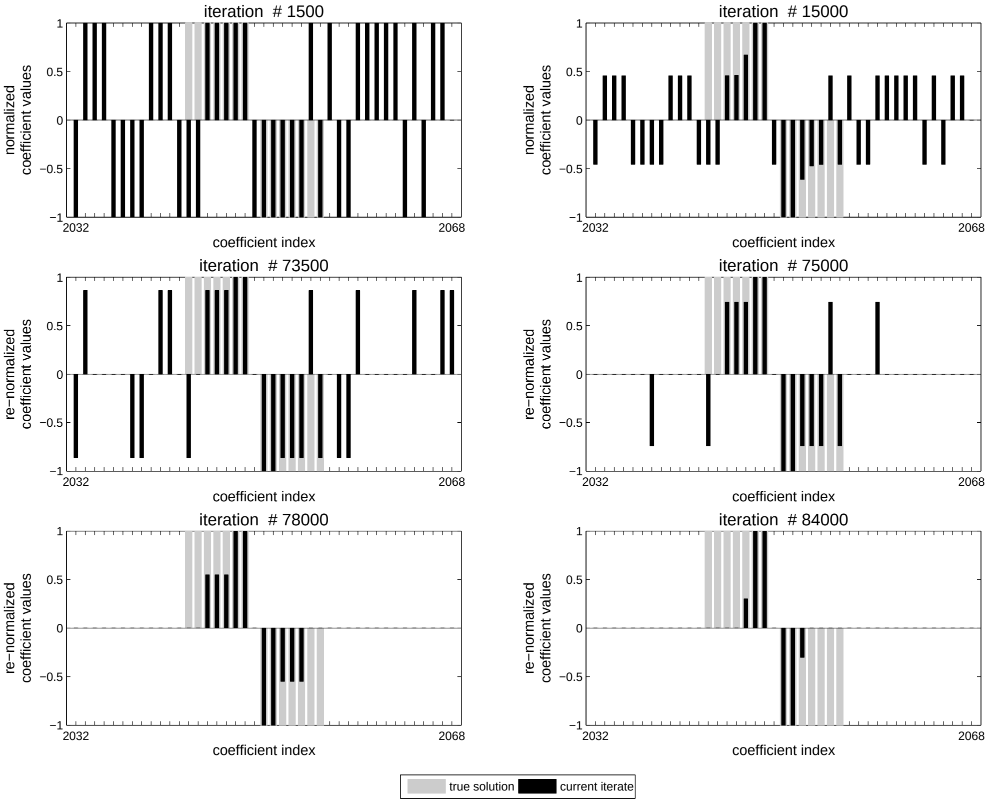

FIGURE 7.3. *The six charts show the progress of the support for the iterations* 1500*,* 15000*,* 73500*,* 75000*,* 78000*, and* 84000 *in the above test example for* $p = 0.4$ *and* $q = 2$*. Only normalized values of coefficients greater than* 10^{-6} *are plotted. Moreover the coefficients of the original coefficients* $x^{\dagger}$ *are highlighted. Bars of the current iterate are additionally scaled with respect to the intermediate iterate after* 1500 *for the first row (iteration* 1500 *and* 15000*) and with respect to the intermediate iterate after* 30000 *iterations for the remaining plots for better visualization.*

normalized with respect to the iterate after 1500 iterations, i.e., the iterate x_{1500} is taken as a reference and the subsequent iterates are scaled with respect to x_{1500}. As some coefficients become very small, we “re-normalize” the values of the coefficients of the iterate after 3000 iterations for the remaining four plots. We observe that the support of the final iterate is contained in the support of the true solution. Moreover, the individual coefficients outside the support decrease monotonously.

We now address the choice of q, as it directly affects the algorithm. In [39] it was shown that the solution to (5.4) can be calculated analytically for $q = 2$. Consequently, the computational effort is reduced significantly at the expense of numerical artifacts in the case of $q = 2$. Figure 7.4 shows the number of (nonzero) entries above a certain threshold in the cases of $q = 1.1, 1.4$, and $q = 2$. As one expects from the theory (cf. Sections 2–5), the choice of $q \in (1, 2)$ has no effect on the solution. In particular, no small nonzero entries occur. For $q = 2$, structurally the same solution is obtained, however, due to numerical artifacts there is an increasing number of small coefficients with respect to the thresholds of 10^{-1}, 10^{-2}, 10^{-7}, 10^{-9}, and 10^{-11}. These effects can be controlled by stringent error criteria, which were relaxed by a factor of 10^{-3} for the results in Figure 7.4. Eventually, one can conclude that the choice of $q = 2$ reduces the computational effort but requires more stringent error criteria if small artifacts should be prevented.

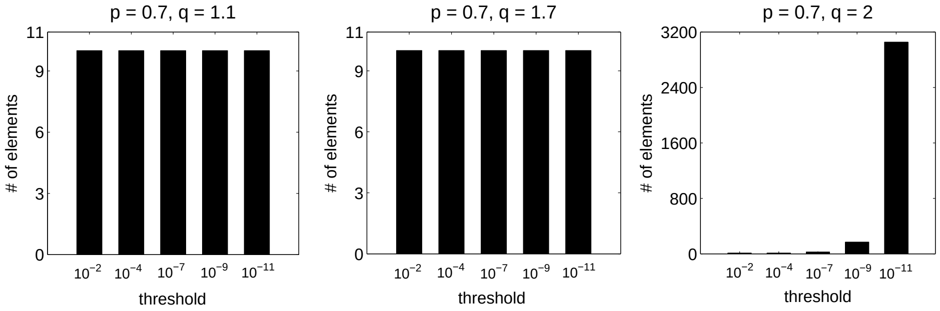

FIGURE 7.4. *The bar charts show the number of (nonzero) entries above the thresholds* $10^{-2}, 10^{-4}, 10^{-7}, 10^{-9}$ *and* 10^{-11}*, for* $q = 1.1, 1.4, 2$ *and* $p = 0.7$*.*

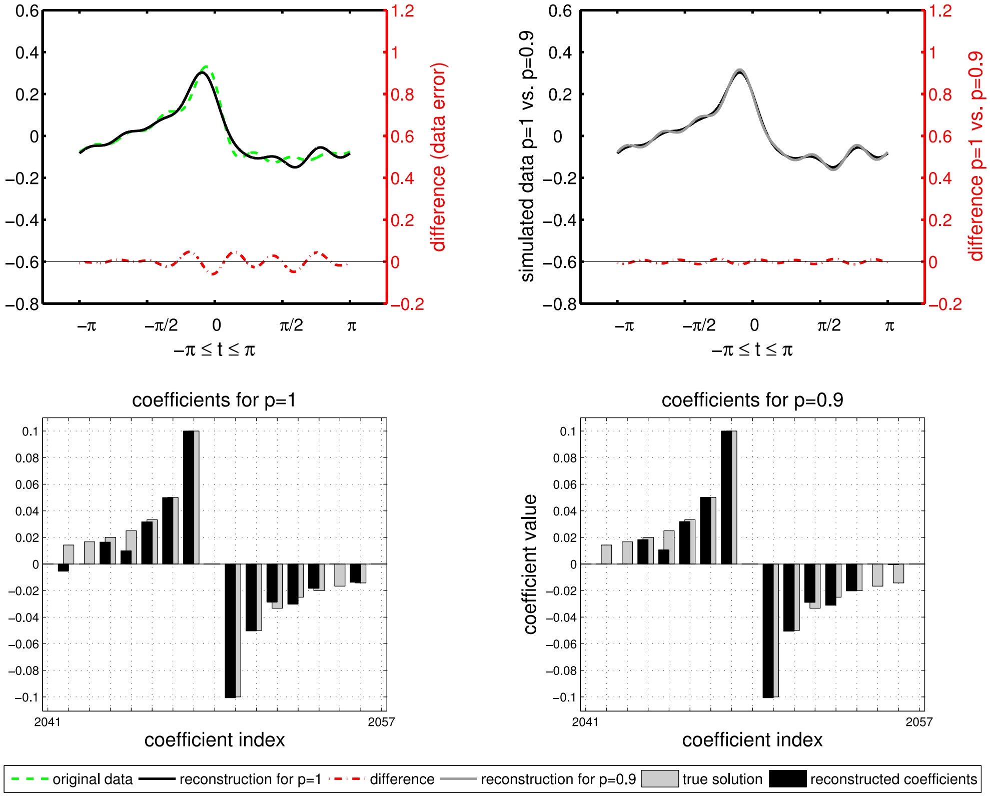

FIGURE 7.5. *In the upper left corner the data fit obtained by the* ℓ_1*-surrogate approach is shown, similarly to Figure 7.2. On the upper right plot the* ℓ_1*-reconstruction is plotted against the obtained reconstruction for* $p = 0.9$ *and* $q = 2$*. Below, the reconstructed coefficients are compared to the true solution for the two cases of* $p = 1$ *and* $p = 0.9$*.*

Finally we compare the classical surrogate algorithm for $p = 1$ with the approach proposed here. In particular, we compare the results obtained for $p = 0.9$ and $q = 2$ with the case of $p = 1$, as they are presumably most similar. In Figure 7.5 we show the data fit obtained by the ℓ_1-approach and compare this with the result presented above for the choice $p = 0.9$ and $q = 2$. We observe that the quality of the obtained data fit is more or less identical and even slightly improved for $p = 0.9$. However, one may notice that the reconstructed coefficient vector is sparser for $p = 0.9$ than for $p = 1$. We observe 12 nonzero elements for the case of $p = 0.9$ and 13 nonzero elements for $p = 1$. Moreover, although all identified coefficients lie within the support of the true solution in the case of $p = 1$, we observe that the reconstructed coefficient with index 2042 (most left coefficient in the lower left bar chart) has the wrong sign compared to the true solution. Eventually, the shown comparison and the results presented for the cases of $p = 0.4, 0.5$, and $p = 0.7$ (see Figure 7.2) indicate an approximation of the classical ℓ_1-surrogate approach for increasing p, which we would also expect from the theory.

In summary, the numerical deconvolution example confirms our analytical findings on the utilization of the transformation operator, the stable convergence, and convergence rates. Additionally, the fact that the reconstructed solutions are always close to the true solution suggests that the algorithm reconstructs the global minimizer fitting the constructed data and thus provides a reconstruction of good quality. Moreover, the strong sparsity promoting feature of the considered regularization functionals and the principle idea of exploiting the transformation operator in numerical algorithms is confirmed. Furthermore, the comparison with the classical ℓ_1-surrogate approach suggests that the proposed approach can be seen as an extension of the ℓ_1-surrogate algorithm with even increased sparsity promoting features. This allows a first rough assessment of the proposed algorithm within the framework of other sparsity promoting algorithms; cf. [2, 4, 32]. However, we would like to emphasize that these algorithms exclusively work for $p \geq 1$ and hence are not directly comparable.

7.2. Parameter Identification for a chemical reaction system — the chlorite-iodide reaction.

The second test example was taken from an application in physical chemistry. We demonstrate the advantages and capabilities of the suggested algorithm for a real world problem. In [30], Kügler et al. use sparsity promoting regularization for a parameter identification problem in a chemical reaction system, the so-called chlorite-iodide reaction. This very well described chemical reaction network provides an attractive test example for the approach considered here. There are several motivations to enforce sparsity when identifying parameters in biological or chemical reaction systems; cf. [21, 30]. First of all, one may address the issue of manageable interpretations of the typically large networks. By identifying the most crucial parameters still explaining the observed dynamics, one can obtain a reduced reaction network in the sense of model reduction. Secondly, the occurring species in these networks typically are not accessible to experimental measurements. Hence, one inevitably lacks information and may encounter unidentifiable parameters. The sparsity promoting regularization is of particular interest as it eliminates those unidentifiable parameters. They become zero, typically leading to zero rates or binding kinetics and hence eliminate the respective reaction terms or species from the network. This is also in accordance with Ockham‘s razor stating that the minimal solution is typically the most likely one. Especially when considering model based approaches, this provides an attractive alternative to quantify these models by means of experimental data and reducing the probable model errors at the same time. Another application for sparsity promoting regularization arises for biological or chemical reaction systems if we consider an already quantified model and want to incorporate additional data or different experimentally observed dynamics. By using the given parameter set as a prior in the regularization term, we promote those solutions with a minimal number of changed parameters. In this way, previously identified parameters are not likely to change and moreover one might identify those mechanisms relevant for the newly observed data or dynamics.

The full chemical reaction system for the chlorite-iodide reaction consists of a system of 7 nonlinear ODEs with 22 parameters as shown below.

$$
\begin{aligned}
\frac{\mathrm{d}[ClO_2]}{\mathrm{d}t} &= -k_1\, ClO_2\, I^- + k_0\, INClO_2 - k_0\, ClO_2 \\
\frac{\mathrm{d}[HOCl]}{\mathrm{d}t} &= k_3\, HClO_2\, I^- + k_4\, HClO_2\, HOI + k_5\, HClO_2\, HIO_2 - k_6\, HOCl\, I^- \\
&\quad - k_7\, HOCl\, HIO_2 - k_0\, HOCl \\
\frac{\mathrm{d}[HIO_2]}{\mathrm{d}t} &= k_4\, HClO_2\, HOI - k_5\, HClO_2\, HIO_2 - k_7\, HOCl\, HIO_2 - k_{8f}\, HIO_2\, I^-\, H \\
&\quad + k_{8r}\, HOI^2 - 2\, k_9\, HIO_2^2 - k_{10}\, HIO_2\, H_2OI^+ - k_0\, HIO_2 \\
\frac{\mathrm{d}[TClO_2^-]}{\mathrm{d}t} &= k_1\, ClO_2\, I^- - k_3\, HClO_2\, I^- - k_4\, HClO_2\, HOI - k_5\, HClO_2\, HIO_2 \\
&\qquad - k_0\, TClO_2^- \\
\frac{\mathrm{d}[THOI]}{\mathrm{d}t} &= k_{2af}\, I_2/H - k_{2ar}\, HOI\, I^- + k_{2bf}\, I_2 - k_{2br}\, H2OI^+\, I^- + k_3\, HClO_2\, I^- \\
&\quad - k_4\, HClO_2\, HOI + k_6\, HOCl\, I^- + 2\, \left(k_{8f}\, HIO_2\, I^-\, H - k_{8r}\, HOI^2\right) \\
&\qquad + k_9\, HIO_2^2 - k_{10}\, HIO_2\, H_2OI^+ - k_0\, THOI \\
\frac{\mathrm{d}[TI^-]}{\mathrm{d}t} &= -k_1\, ClO_2\, I^- + k_{2af}\, I_2/H - k_{2ar}\, HOI\, I^- + k_{2bf}\, I_2 - k_{2br}\, H_2OI^+\, I^- \\
&\quad - k_3\, HClO_2\, I^- - k_6\, HOCl\, I^- - k_{8f}\, HIO_2\, I^-\, H + k_{8r}\, HOI^2 \\
&\qquad + k_{10}\, HIO_2\, H_2OI^+ + k_0\, INI^- - k_0\, TI^- \\
\frac{\mathrm{d}[TI_2]}{\mathrm{d}t} &= 0.5\, k_1\, ClO_2\, I^- - k_{2af}\, I_2/H + k_{2ar}\, HOI\, I^- - k_{2bf}\, I_2 + k_{2br}\, H_2OI^+\, I^- \\
&\qquad - k_0\, TI_2,
\end{aligned}
$$

where

$$
\begin{aligned}
I^- &= TI^- - (K_{16} + TI^- + TI_2)/2 - \sqrt{(K_{16} + TI^- + TI_2)^2/4 - TI^-\, TI_2} \\
I_2 &= TI_2 - (K_{16} + TI^- + TI_2)/2 - \sqrt{(K_{16} + TI^- + TI_2)^2/4 - TI^-\, TI_2} \\
HClO_2 &= TClO_2^- \, \frac{H}{(K_{14} + H)} \\
H_2OI^+ &= THOI\, \frac{H}{(K_{15} + H)} \\
HOI &= THOI\, \frac{K_{15}}{(K_{15} + H)}.
\end{aligned}
$$

Table 7.2 provides a list of the occurring species. The parameters mostly denote reaction rates or binding constants, which are assumed to be constant for the experiment. For an exact derivation and explanation of the species and parameters, we refer to [30]. Eventually, the experimental setup can be formulated by means of the shown ODE system and the algebraic equations below.

The chlorite-iodide reaction is a so-called “chemical clock” and therefore exhibits sudden rapid changes in the compound concentration. This causes the mathematical ODE model to be highly nonlinear and stiff and consequently increases the computational load. We use the adjoint state technique for an efficient calculation of the gradient of the objective. Furthermore, we consider only a single data set, i.e., we assume the pH-value to be constant; cf. [30].

TABLE 7.2

The table shows the molecular formulas and names of the species occurring in the considered model of the chlorite-iodide reaction system.

molecular formula	name
ClO_2	chlorine dioxide
$HOCl$	hypochlorous acid
HIO_2	iodous acid
ClO_2^-	chlorite ion
HOI	hypoiodous acid
I^-	iodide ion
I_2	iodine
$HClO_2$	chlorous acid
H_2OI^+	protonated hypoiodous acid

Naturally, this is likely to reduce the number of identifiable parameters. In accordance with the findings in [30], we subsequently present even sparser solutions for the single data set. The data were generated based on the results presented in [30]. In this way, we obtain a reasonable size of the problem (i.e., identifying all parameters by means of the time course of the ODE species from a single experiment) with realistic parameters and known true solution and an added relative noise level of about five percent. In order to reduce the computational load, we first identify a parameter set by means of a standard ℓ_2-regularization. The obtained solution is then used as an initial guess. Furthermore, the solution can be used for an efficient weighting of the regularization term for all nonzero coefficients of the ℓ_2-solution. This is essential, as the parameters of the chemical model vary on a scale of more than 10^{20}. With the exception of the second coefficient, all parameters obtained by the ℓ_2-fit are nonzero and have been used for weighting.

In the first experiment we chose the algorithmic parameters $p = 0.7$ and $q = 1.2$. Figure 7.6 displays the obtained reconstruction in this case, which provides a rather good fit particularly with regard to the occurring rapid changes.

The next Figure 7.7 depicts the identified parameters, where 8 out of 17 parameters are different from zero. Note that some parameters are rather large, which is to be expected as large values are decreasingly penalized for our regularization method. Consequently, this solution significantly differs from the true solution concerning the magnitude of the individual parameters. However, note that all nonzero coefficients in the computed solution are part of the support of the true solution. In particular, except for the parameter K_{16}, which is zero in our identified parameter set, the support of the computed and the true solution are identical.

In order to assess this result concerning the sparsity promoting features, we compare it with the reconstruction obtained for the case $p = 1$ and $q = 1$. Figure 7.8 shows the data fit, which exhibits a similar quality as obtained in the case $p = 0.7$ and $q = 1.2$. Nevertheless, the identified parameters essentially differ from the ones shown in Figure 7.7.

Figure 7.9 displays the computed solution using the ℓ_1-penalization term. We observe that the nonzero parameters only lie within the support of the true solution. In fact, for the depicted solution, the support is identical with the one of the true solution because the parameter K_{16} is nonzero in this case. Hence, we observe again an enhanced sparsity promoting effect by means of the non-convex regularization method. Note that for the solution shown in Figure 7.9, the size of the parameters varies less and is closer to one, i.e., to the initial guess/weights.

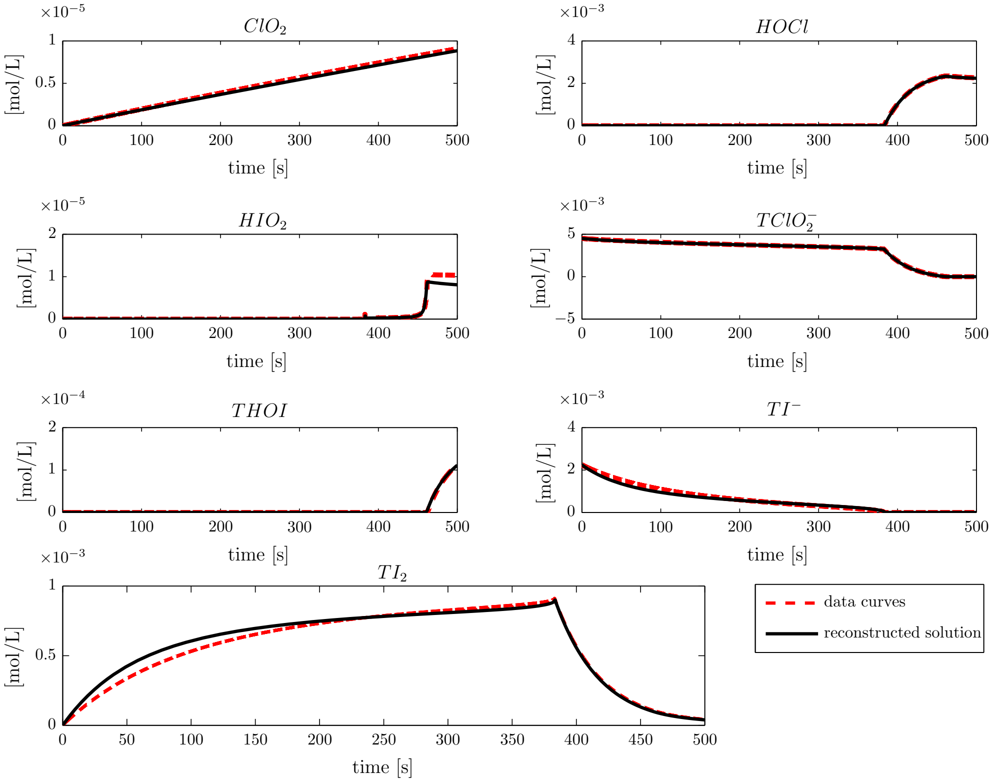

FIGURE 7.6. *Concentration of the ODE species obtained by sparsity promoting regularization with* $p = 0.7$ *and* $q = 1.2$*.*

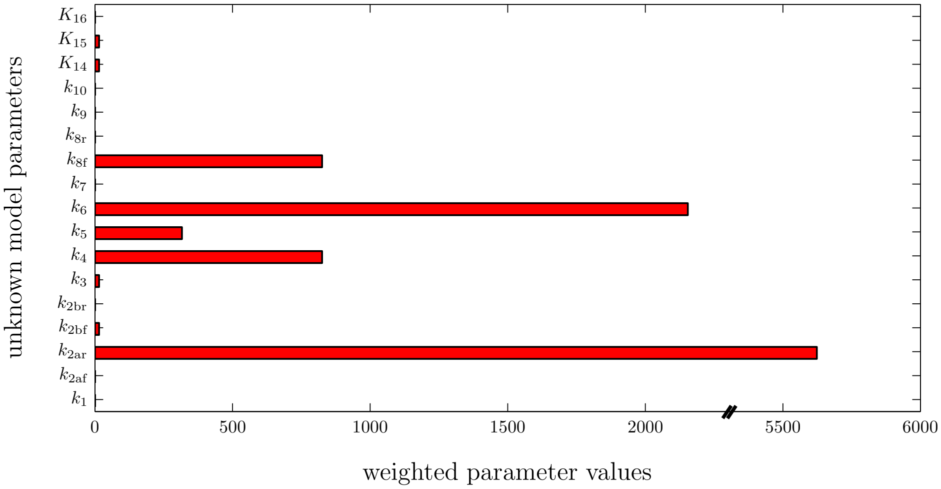

FIGURE 7.7. *Parameters identified for the chlorite-iodide reaction system with* $p = 0.7$ *and* $q = 1.2$ *and weighted with respect to the initial guess.*

As it is also observed for the deconvolution problem, our algorithm shows a stable convergence for the nonlinear problem. However, we have observed an increased computational effort due to the highly nonlinear operator. In particular, local minima increase the overall

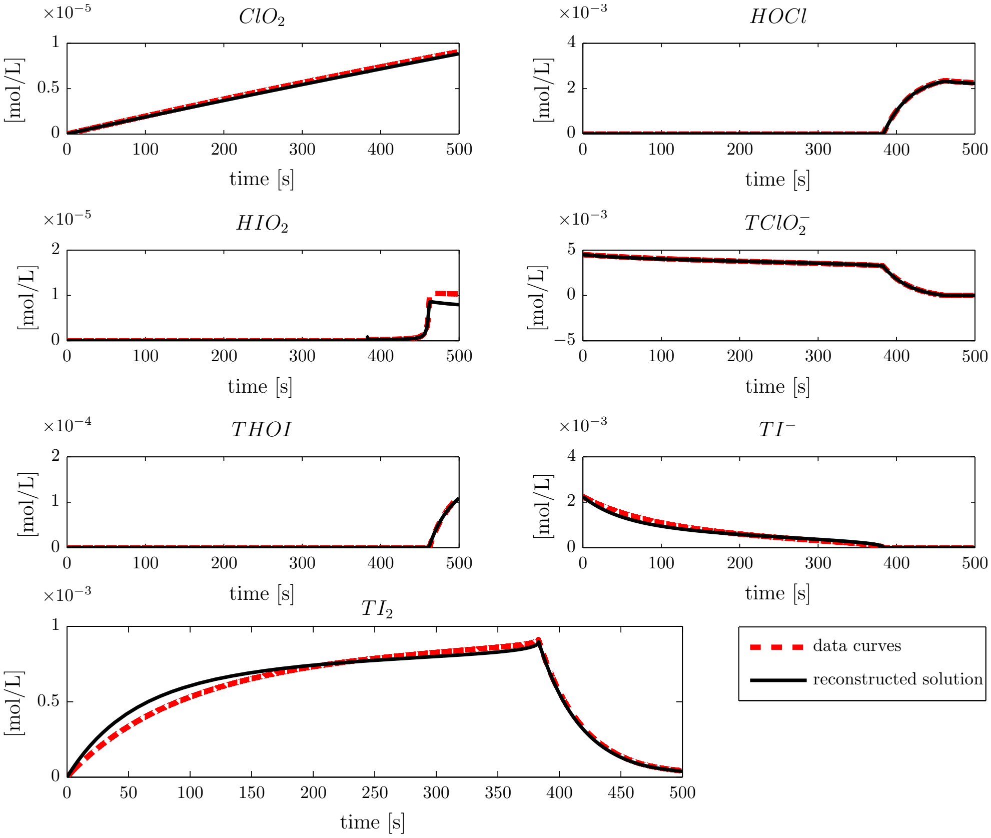

FIGURE 7.8. *Concentration of the ODE species obtained by sparsity promoting regularization with* $p = 1$ *and* $q = 1$.

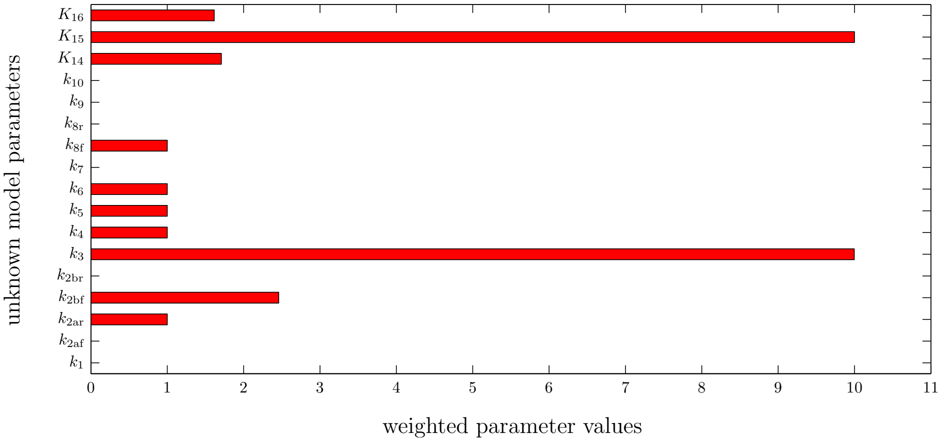

FIGURE 7.9. *Parameters identified for the chlorite-iodide reaction system with* $p = 1$ *and* $q = 1$.

computation time and we have found an even increased sensitivity with respect to the choice of the regularization parameter. Therefore we use a very fine grid for the different values of α $(0.9^{\{0,1,2,\ldots,\}})$. The fine grid for α and the addressed stiff and nonlinear character of the considered ODE system required an efficient ODE solver. The evaluation time of the forward operator and the computation time of the gradient strongly depended on the respective parameter set and the current iterate. To reduce the computation time, we used the CVODES ODE solver library from SUNDIALS. Usually the evaluation of the forward operator takes a few milliseconds up to some seconds, whereas the computation time for the gradient is typically slightly increased and lies between some milliseconds and up to several seconds. The use of the SUNDIALS package decreases the computation time about thirty percent. Moreover, one may note that only non-negative values for the concentration of the species and the parameter values are realistic and acceptable. However due to numerical artifacts, negative values might occur during the ODE integration. We control this by stringent absolute error tolerances for the solver as suggest by the developers of the solver library.

In summary, we can conclude that the proposed algorithm provides a reasonable extension of the surrogate approach for non-convex sparsity promoting regularization terms in sequence spaces. It was successfully applied to the deconvolution problem leading to a linear operator equation, as well as to the parameter identification problem with a highly nonlinear operator. In both cases, a strong sparsity promoting feature was observed. Moreover, we showed that the technique of the transformation operator potentially allows to transform the ℓ_p-regularization problem for $p < 1$ to a general ℓ_q-problem with $q \geq 1$. This is especially of interest as numerous techniques for ℓ_q-regularization with $q \geq 1$ exist, which can then be utilized. In particular, methods which have already been shown to have sparsity promoting features (e.g., ℓ_1-regularization) provide attractive iterative schemes. The transformation operator technique then would act as a sparsity enhancing map. For our future work, we plan to investigate those possibilities and analyze the impact of the transformation operator.

Acknowledgments. R. Ramlau acknowledges support of this work by the FWF Grants P19496-N18 and P20237-N14. C. A. Zarzer thanks H. W. Engl for his support and supervision and P. Kügler for his support and many fruitful discussions. C. A. Zarzer acknowledges support by the WWTF Grant MA07-030.

REFERENCES

[1] S. W. Anzengruber and R. Ramlau, *Morozov's discrepancy principle for Tikhonov-type functionals with nonlinear operators*, Inverse Problems, 26 (2010), 025001 (17 pages).
[2] A. Beck and M. Teboulle, *A fast iterative shrinkage-thresholding algorithm for linear inverse problems*, SIAM J. Imaging Sci., 2 (2009), pp. 183–202.
[3] J. Bect, L. Blanc-Féraud, G. Aubert, and A. Chambolle, *A l^1-unified variational framework for image restoration*, in Computer Vision–ECCV 2004, Proceedings of the 8th European Conference on Computer Vision, Prague, T. Pajdla, J. Matas, eds., Lecture Notes in Computer Science, 3024, Springer, Berlin, 2004, pp. 1–13.
[4] J. M. Bioucas-Dias and M. A. T. Figueiredo, *A new TwIST: two-step iterative shrinkage/thresholding algorithms for image restoration*, IEEE Trans. Image Process., 16 (2007), pp. 2992–3004.
[5] T. Bonesky, K. Bredies, D. A. Lorenz, and P. Maass, *A generalized conditional gradient method for nonlinear operator equations with sparsity constraints*, Inverse Problems, 23 (2007), pp. 2041–2058.
[6] K. Bredies and D. A. Lorenz, *Iterated hard shrinkage for minimization problems with sparsity constraints*, SIAM J. Sci. Comput., 30 (2008), pp. 657–683.
[7] ———, *Linear convergence of iterative soft-tresholding*, J. Fourier Anal. Appl., 14 (2008), pp. 813–837.
[8] K. Bredies, D. Lorenz, and P. Maass, *A generalized conditional gradient method and its connection to an iterative shrinkage method*, Comput. Optim. Appl., 42 (2009), pp. 173–193.
[9] E. Candes, J. Romberg, and T. Tao, *Stable signal recovery from incomplete and inaccurate measurements*, Comm. Pure Appl. Math, 59 (2006), pp. 1207–1223.
[10] E. Candes and T. Tao, *Decoding by linear programming*, IEEE Trans. Inform. Theory, 51 (2005), pp. 4203–4215.
[11] ———, *Near-optimal signal recovery from random projections: universal encoding strategies?*, IEEE Trans. Inform. Theory, 52 (2006), pp. 5406–5425.
[12] I. Cioranescu, *Geometry of Banach spaces, Duality Mappings and Nonlinear Problems*, Kluwer, Dordrecht, 1990.

[13] A. COHEN, W. DAHMEN, AND R. DEVORE, *Compressed sensing and best k-term approximation*, J. Amer. Math. Soc., 22 (2009), pp. 211–231.
[14] P. L. COMBETTES AND V. R. WAJS, *Signal recovery by proximal forward-backward splitting*, Multiscale Model. Simul., 4 (2005), pp. 1168–1200.
[15] I. DAUBECHIES, M. DEFRISE, AND C. DE MOL, *An iterative thresholding algorithm for linear inverse problems with a sparsity constraint*, Comm. Pure Appl. Math., 57 (2004), pp. 1413–1457.
[16] I. DAUBECHIES, R. DEVORE, M. FORNASIER, AND S. GÜNTÜRK, *Iteratively reweighted least squares minimization for sparse recovery*, Comm. Pure Appl. Math., 63 (2010), pp. 1–38.
[17] D. DONOHO, *Compressed sensing*, IEEE Trans. Inform. Theory, 52 (2006), pp. 1289–1306.
[18] ———, *High-dimensional centrally symmetric polytypes with neighborliness proportional to dimension*, Discrete Comput. Geom., 35 (2006), pp. 617–652.
[19] D. DONOHO AND P. STARK, *Uncertainty principles and signal recovery*, SIAM J. Appl. Math., 49 (1989), pp. 906–931.
[20] D. DONOHO AND J. TANNER, *Sparse nonnegative solutions of underdetermined linear equations by linear programming*, Proc. Natl. Acad. Sci. USA, 102 (2005), pp. 9446–9451.
[21] H. W. ENGL, C. FLAMM, P. KÜGLER, J. LU, S. MÜLLER, AND P. SCHUSTER, *Inverse problems in systems biology*, Inverse Problems, 25 (2009), 123014 (51 pages).
[22] H. W. ENGL AND G. LANDL, *Convergence rates for maximum entropy regularization*, SIAM J. Numer. Anal., 30 (1993), pp. 1509–1536.
[23] M. FORNASIER, R. RAMLAU, AND G. TESCHKE, *The application of joint sparsity and total variation minimization algorithms to a real-life art restoration problem*, Adv. Comput. Math., 31 (2009), pp. 157–184.
[24] M. GRASMAIR, *Well-posedness and convergence rates for sparse regularization with sublinear l^q penalty term*, Inverse Probl. Imaging, 3 (2009), pp. 383–387.
[25] ———, *Non-convex sparse regularisation*, J. Math. Anal. Appl., 365 (2010), pp. 19–28.
[26] M. GRASMAIR, M. HALTMEIER, AND O. SCHERZER, *Sparse regularization with l^q penalty term*, Inverse Problems, 24 (2008), 055020 (13 pages).
[27] ———, *Necessary and sufficient conditions for linear convergence of ℓ^1-regularization*, Comm. Pure Appl. Math., 64 (2011), pp. 161–182.
[28] R. GRIBONVAL AND M. NIELSEN, *Highly sparse representations from dictionaries are unique and independent of the sparseness measure*, Appl. Comput. Harmon. Anal., 22 (2007), pp. 335–355.
[29] R. GRIESSE AND D. LORENZ, *A semismooth Newton method for Tikhonov functionals with sparsity constraints*, Inverse Problems, 24 (2008), 035007 (19 pages).
[30] P. KÜGLER, E. GAUBITZER, AND S. MÜLLER, *Parameter identification for chemical reaction systems using sparsity enforcing regularization: a case study for the chlorite–iodide reaction*, J. Phys. Chem. A, 113 (2009), pp. 2775–2785.
[31] D. A. LORENZ, *Convergence rates and source conditions for Tikhonov regularization with sparsity constraints*, J. Inverse Ill-Posed Probl., 16 (2008), pp. 463–478.
[32] I. LORIS, M. BERTERO, C. DE MOL, R. ZANELLA, AND L. ZANNI, *Accelerating gradient projection methods for l_1-constrained signal recovery by steplength selection rules*, Appl. Comput. Harmon. Anal., 27 (2009), pp. 247–254.
[33] M. NIKOLOVA, *Markovian reconstruction in computed imaging and Fourier synthesis*, in Proceedings of the 2004 International Conference on Image Processing 1994, ICIP–94, IEEE Conference Proceedings, pp. 690–694.
[34] R. PYTLAK, *Conjugate Gradient Algorithms in Nonconvex Optimization*, Springer, Berlin, 2009.
[35] R. RAMLAU, *A steepest descent algorithm for the global minimization of the Tikhonov functional*, Inverse Problems, 18 (2002), pp. 381–405.
[36] ———, *TIGRA—an iterative algorithm for regularizing nonlinear ill–posed problems*, Inverse Problems, 19 (2003), pp. 433–467.
[37] ———, *Regularization properties of Tikhonov regularization with sparsity constraints*, Electron. Trans. Numer. Anal., 30 (2008), pp. 54–74.
`http://etna.mcs.kent.edu/vol.30.2008/pp54-74.dir`
[38] R. RAMLAU AND E. RESMERITA, *Convergence rates for regularization with sparsity constraints*, Electron. Trans. Numer. Anal., 37 (2010), pp. 87–104.
`http://etna.mcs.kent.edu/vol.37.2010/pp87-104.dir`
[39] R. RAMLAU AND G. TESCHKE, *Tikhonov replacement functionals for iteratively solving nonlinear operator equations*, Inverse Problems, 21 (2005), pp. 1571–1592.
[40] ———, *A Tikhonov-based projection iteration for nonlinear ill-posed problems with sparsity constraints*, Numer. Math., 104 (2006), pp. 177–203.
[41] ———, *An iterative algorithm for nonlinear inverse problems with joint sparsity constraints in vector-valued regimes and an application to color image inpainting.*, Inverse Problems, 23 (2007), pp. 1851–1870.
[42] ———, *Sparse recovery in inverse problems*, in Theoretical Foundations and Numerical Methods for Sparse Recovery, M. Fornasier, ed., Radon Series on Computational and Applied Mathematics 9, De Gruyter,

Berlin, 2010, pp. 201–262.
[43] O. SCHERZER, *A modified Landweber iteration for solving parameter estimation problems*, Appl. Math. Optim., 38 (1998), pp. 45–68.
[44] S. WRIGHT, R. NOWAK, AND M. FIGUEIREDO, *Sparse reconstruction by separable approximation*, IEEE Trans. Signal Process., 57 (2009), pp. 2479–2493.
[45] C. A. ZARZER, *On Tikhonov regularization with non-convex sparsity constraints*, Inverse Problems, 25 (2009), 025006 (13 pages).
[46] C. A. ZARZER, *Sparsity Enforcing Regularization on the* ℓ_p*-Scale With* $p < 1$, Ph.D. Thesis, Industrial Mathematics Institute, Johannes Kepler University Linz, 2012.